



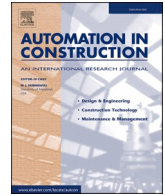
## **Digital tool integrations for architectural reuse of salvaged building materials**

Downloaded from: <https://research.chalmers.se>, 2025-01-20 01:30 UTC

Citation for the original published paper (version of record):

Zboinska, M., Göbel, F. (2025). Digital tool integrations for architectural reuse of salvaged building materials. *Automation in Construction*, 170. <http://dx.doi.org/10.1016/j.autcon.2024.105947>

N.B. When citing this work, cite the original published paper.



# Digital tool integrations for architectural reuse of salvaged building materials

Malgorzata A. Zboinska<sup>\*</sup>, Frederik Göbel

Department of Architecture and Civil Engineering, Chalmers University of Technology, SE-412 96 Gothenburg, Sweden

## ARTICLE INFO

### Keywords:

Architectural reuse  
Salvaged construction materials  
Digital twins  
Photogrammetry  
Robot vision  
Computer vision  
Machine learning  
Robotic fabrication  
3D printing  
Data-driven toolpath design

## ABSTRACT

Building material reuse can reduce the environmental impact of construction yet its advanced digital support is still limited. Which digital tools could effectively support repair of highly irregular, salvaged materials? To probe this question, a framework featuring six advanced digital tools is proposed and verified through six design and prototyping experiments. The experiments demonstrate that a digital toolkit integrating photogrammetry, robot vision, machine learning, computer vision, computational design, and robotic 3D printing effectively supports repair and recovery of irregular reclaimed materials, enabling their robust digitization, damage detection, and feature-informed computational redesign and refabrication. These findings contribute to the advancement of digitally aided reuse practices in the construction sector, providing valuable insights into accommodating highly heterogeneous reclaimed materials by leveraging advanced automation and digitization. They provide the crucial and currently missing technological and methodological foundation needed to inform future research on industrial digital solutions for reuse.

## 1. Introduction

The construction of buildings profoundly impacts the natural environment, leading to excessive waste generation and greenhouse gas emissions. More efficient utilization of existing materials in the built environment can significantly lower these negative effects [1]. Therefore, a new architectural design practice based on the reuse of materials salvaged from demolished buildings is emerging today. Capitalizing on existing material stocks, it aims to diminish the need for new material production and thereby lower the environmental impact of construction [2]. Due to its accelerating importance, this practice is now in need of feasible methods, workflows, and application examples that will help to propel its proliferation in the construction sector.

One of the significant challenges of reuse is the non-standard character of reclaimed materials and elements [3,4]. They are usually highly heterogeneous, differing in dimensions, form, and appearance because they often become damaged during dismantling, and may originate from different buildings. This makes it more difficult to reassemble them into coherent new configurations. Thus, materials and components exhibiting a high level of differentiation and damage can often be disqualified from reuse and unnecessarily become construction waste [5]. In some cases, component irregularity is mitigated by applying large

modifications, such as cutting and milling, to standardize the elements' dimensions and joinery details. However, this approach also produces waste [6].

Thus, is the most resource-efficient reuse scenario, the reclaimed materials and components should be incorporated in a waste-free manner, to bypass the abovementioned challenges. Such an approach requires access to detailed data describing the characteristics of each reclaimed element, to enable a precise design process involving repair and accommodation in new architectural contexts [7]. Today's advanced digital tools and technologies offer the possibility of not only the acquisition of such precise data but also of using this data to support the entire circular design process [8]. Specifically, digital capture techniques such as photogrammetry, 3D scanning, and machine vision enable precise registration of the finest details of any building component in a digital format [9–11]. This data can be stored as 2D raster images, 3D point clouds, and mesh-based digital twin models, providing access to information about each element's size, geometry, color, and surface features. Further, computer vision (CV) methods, machine learning (ML) algorithms, and custom computational design routines enable agile management, filtering, and utilization of this data for design purposes [12–14]. If coupled with digital manufacturing techniques, such as robotic fabrication, they facilitate direct and effective

<sup>\*</sup> Corresponding author.

E-mail address: [malgorzata.zboinska@chalmers.se](mailto:malgorzata.zboinska@chalmers.se) (M.A. Zboinska).

transitions from design to realization [15]. Thus, once combined into a larger digital toolkit, these solutions promise to effectively support the accommodation of salvaged components through precise, zero-waste design and production.

Despite the promising potential of each of these tools, examples of their combined use reported in research literature are scarce. So far, the tools were applied in limited configurations, and, in most cases, these applications were not meant to support reuse. For instance, the combination of machine learning and robotic fabrication was proposed to demonstrate its potential for automating and informing digital manufacturing routines by using real-time data about the dynamic behavior of processed materials [13,15,16]. Integrations of robot vision and 3D printing have been shown to inform the fabrication processes of architectural structures with free-form shapes [17]. The further coupling of these two techniques with machine learning was also proven useful in the prediction, planning, and automatic generation of robotic additive manufacturing paths and the design of robotic assembly sequences [18–20]. Finally, a limited number of papers reported on the integrations of computer numerically controlled (CNC) milling with data-driven computational design [6,21] as well as 3D scanning [22], to allow for the assembly of uniquely shaped construction materials.

At present, only a few architectural publications discussed digitally aided element treatment, and featured the use of different digital techniques. Among these exceptions, in one paper, digital workflows combining photogrammetry, computational design, CNC milling, and robotic 3D printing were developed to enable the application of restorative biobased coating treatments onto architectural elements from timber [23]. Another publication reported on the use of photogrammetry, computational design, and robotic 3D printing to repair existing biobased composites [24]. Combined use of 3D scanning, parametric design, computational structural analysis, and robotic assembly was also proposed, to facilitate the assembly of structures from off-cut wood [25]. Finally, an integration of ten different digital technologies was also put forth as part of a large, generic framework meant to support the entire circular design process [26]. Therein, the identification of materials for reuse in the built environment was planned to be aided with ML, CV and reality capture techniques, the sourcing of the identified materials using extended reality and robotics, followed by material distribution using digital product passports, internet of things, and blockchain technologies, and ending with the design and production process involving the reused components supported with generative AI, computational design, and digital manufacturing.

Examples of other tool integrations, albeit not the six ones targeted in this paper, and not geared specifically at building material reuse, repair, and renovation, can also be found in adjacent fields. One such field is heritage preservation, where the use of different 3D scanning methods in combination with 3D printing was applied to replicate historical artifacts [27–30]. Another field offering examples of digital technique integrations is product remanufacturing. Therein, the combination of 3D scanning and 3D printing, as well as camera-assisted real-time image processing and ML were used to facilitate product inspection, and then product repair through additive remanufacturing [31,32]. Digital tool integrations can also be found in the field of civil engineering, where 3D scanning and 3D printing were jointly applied to repair cracks in concrete [33], and in geotechnics, where additive and subtractive manufacturing [34], as well as various ML techniques, were combined to better detect, simulate and physically test cracks in solid structures [35,36].

This current state-of-the-art indicates that even if various digital technique integrations have been reported already, there is a knowledge gap concerning specifically the demonstration of an integration that comprehensively supports the process of waste-free treatment of non-standard reclaimed building materials and elements, with architectural reuse as the targeted domain of application. Further, despite the presence of papers in which different digital tool combinations were featured, the specific combination proposed here, integrating

photogrammetry, robot vision, machine learning, computer vision, computational design, and robotic 3D printing, has not been reported yet. Thus, knowledge is missing on how the mentioned tools can be combined to support the architectural reuse process, from design to production, and how they can support diverse architectural scenarios of zero-waste reuse.

Consequently, the main novelty of this paper is in the proposal of a generic digital process framework combining the six digital tools mentioned above: photogrammetry, robot vision, machine learning, computer vision, computational design, and robotic 3D printing. The application of these tools is demonstrated for the first time, in different configurations, and in various scenarios of material treatments, with reuse as an intended realm of application. These scenarios embrace surface repair through new texturing, element damage repair through material infills, and element reassembly by combining reclaimed and new materials. The original feature of the proposed tool integration, compared with the results published so far, resides in its capacity to inform the design process of reuse interventions. Further, in its ability to inform the robotic manufacturing routines accompanying this process through direct engagement of different types of data describing the component features. As such, this integration allows for the redesign and reuse of any component, regardless of its complexity and level of damage, contributing to an increase in the bulk of reclaimed materials that can be reused.

## 2. Methods, materials, and generic digital process framework

The software platform enabling the application of the proposed framework and workflows is Rhinoceros 3D [37] and its visual programming environment Grasshopper [38], well-known in architectural practice and offering extended functionalities through a broad range of open-source add-ons, and the possibility of augmenting user-defined programming modules. These add-ons, as well as custom programs developed and supporting hardware, are specified further on.

The reclaimed architectural elements treated in the experiments embraced eight timber floorboard fragments, harvested from a local demolition site, end exhibiting different types of damage (Fig. 1). The 3D printing interventions applied on these salvaged pieces to enable their reuse were done using filaments containing wood and hemp biomass.

The research method was based on the conceptualization of a generic digital process framework featuring different enabling tools, and the verification and demonstration of its practical application through the conduct of six architectural prototyping experiments. The generic framework comprises three stages: digital data capture, digital processing of the captured data, and data harnessing through the data-driven generation of robotic fabrication sequences (Fig. 2). These stages are discussed in detail below.

### 2.1. Data capture

The first stage in the process framework focuses on digitalizing the physical elements, to acquire the data describing their intricate features in a digital format. Three different data capture methods are included, namely 2D raster image capture using a digital camera, 3D mesh capture through photogrammetry based on the digital photographs of the treated pieces, and 3D point cloud capture using a custom-built robot vision system with a color and depth camera.

In the conducted experiments, the registration of object data in 2D raster images was done using a digital, 12-megapixel camera of the iPhone 11 smartphone (Fig. 3). Each wooden piece was placed on a horizontal neutral background surface. Then, it was photographed in top view, with the camera oriented horizontally to the surface on which the piece was placed. To acquire a digital twin mesh representation of each piece, the photogrammetry technique was employed. Using the same camera as above, photographs of each piece were taken in a 360°

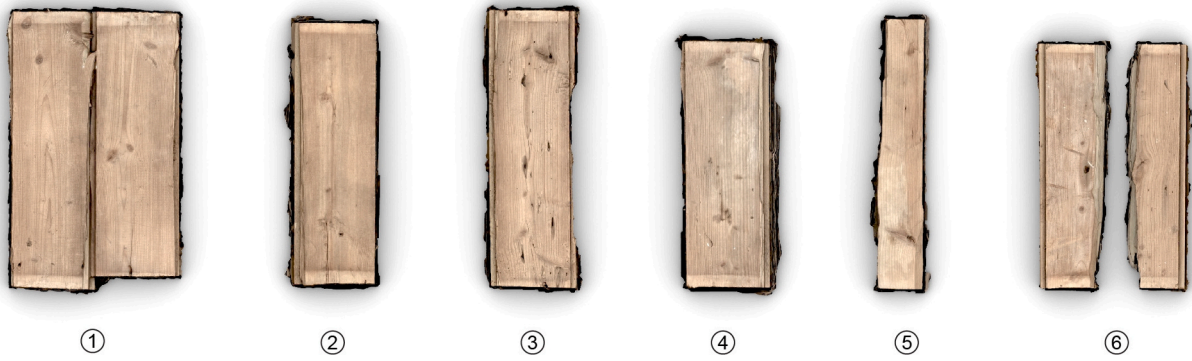


Fig. 1. Overview of reclaimed wooden floorboards undergoing six experimental reuse interventions, presented as textured mesh models captured through photogrammetry.

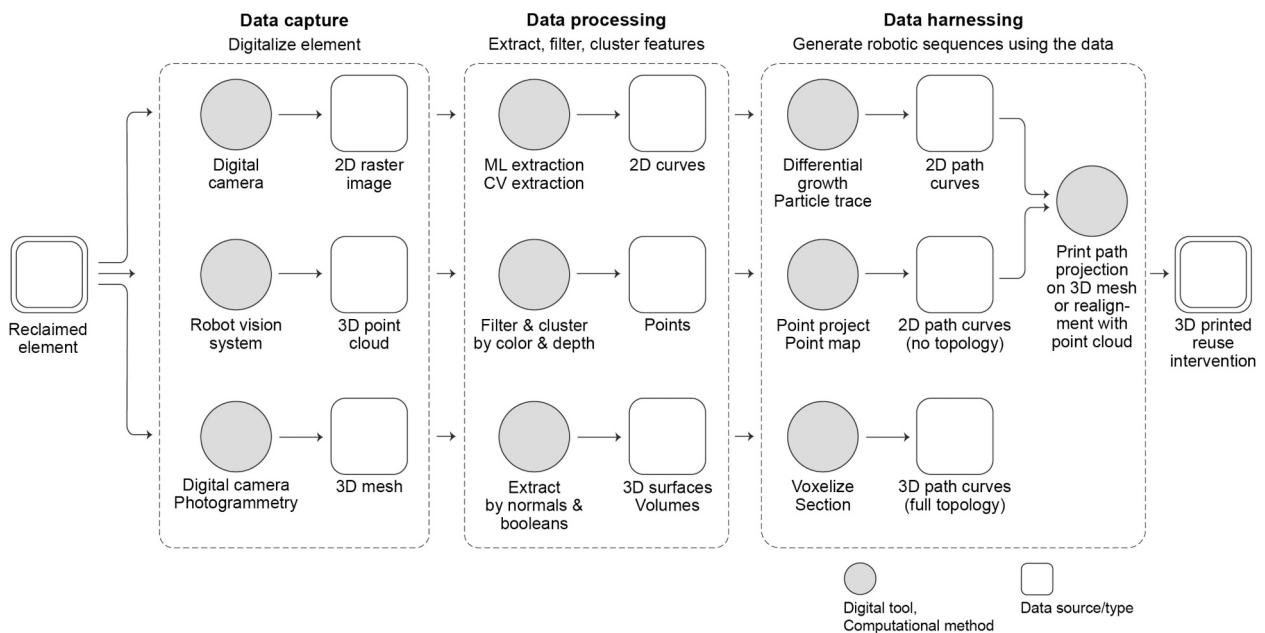


Fig. 2. Digital process framework and enabling tools supporting reuse-oriented design and manufacturing of reclaimed architectural materials.

panoramic range, with approximately 25 % overlap between the photographs. At least three photographing series in the panoramic range were executed at various distances and angles toward the digitalized piece, to ensure that every fragment is registered. For each piece, a total of 200 photographs were taken whereof approximately 25 % were capturing the unique detailed features of the piece. The photographs were then processed using the KIRI Engine app [39] on iPhone 11. In this way, a digital twin model of the piece was acquired as a triangulated mesh in .obj format with accompanying color and texture data in .mtl format.

Finally, to register object features in a 3D point cloud format, a robot vision system based on a structured light-based Polyga V1 camera with RGB color and depth sensors was devised and mounted as an end-effector on an industrial robot KUKA Agilus KR10-R110-SIXX (Fig. 4). The enabling hardware setup comprised the V1 camera, the robot arm manipulator with a custom mounting system for the camera, as well as the E3D Titan Aero extruder for 3D printing. Further, a personal computer (PC), a robot controller KUKA C4 Compact, and a LucidControl 4-channel USB digital input module for monitoring isolated 24 V digital input signals. The digital input of the module was connected to a digital output pin of the robot controller's X12 user interface port. The module and the V1 camera were also connected to the user PC via a USB 3.0

connection.

To facilitate data capture at designated camera locations above the digitalized physical piece, a linear robot movement path with 2 s pauses at predefined locations was programmed in Grasshopper via the KUKA|prc add-in [40]. Upon each pause, a digital output signal set to a true value was sent via the robot program to the robot controller and then to the LucidControl digital input module. The module, through its USB cable connection with the V1 camera, triggered point cloud data capture. This allowed for the capture data to be sent back to Grasshopper via the USB connection. To transform the digital output value from the robot program into an analog signal in the USB connection, a custom Grasshopper component based on the LucidControl .Net Application Programming Interface (API) [41] was developed in C# [42]. To adjust the V1 camera settings and facilitate the receipt of the captured data within Grasshopper, the camera was controlled live using a custom C# code [43]. This code also processed the raw data from the capture into a Grasshopper-compatible data format, represented as lists of points and colors describing the resultant point cloud.

Once the captured data was translated into the Grasshopper format, the Cartesian coordinates of the points, initially expressed in the local coordinate system of the V1 camera, were mapped to be expressed in the world coordinate system values of the Rhinoceros 3D file. This was done

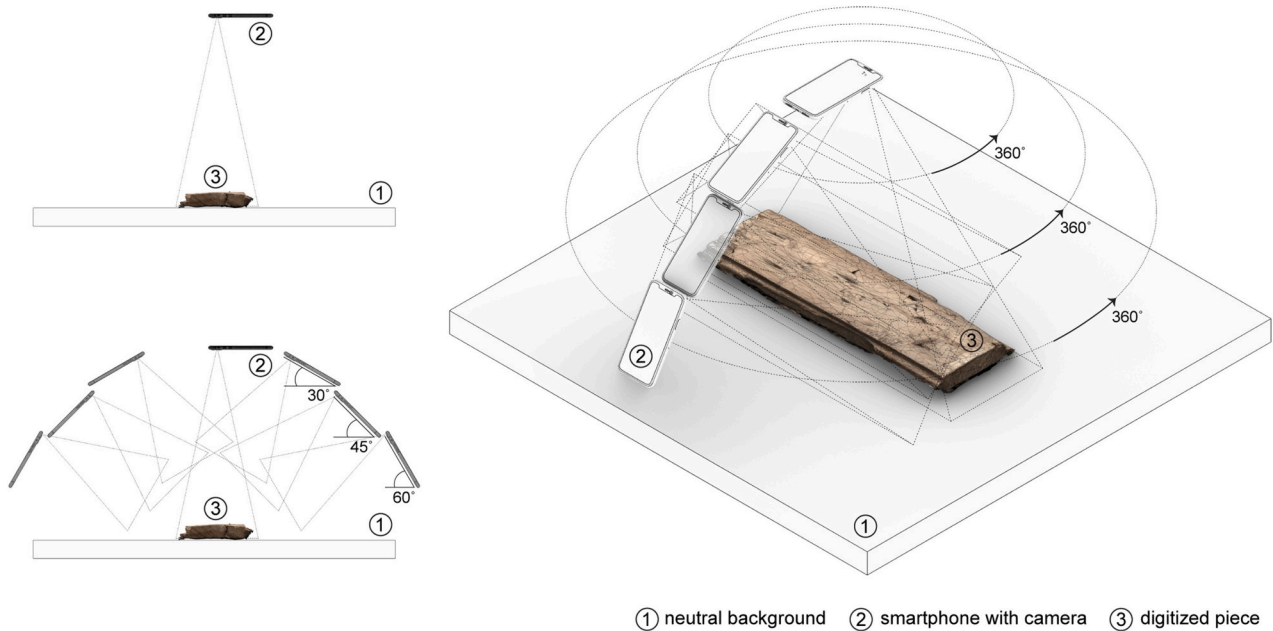


Fig. 3. Setups for 2D raster image capture and photogrammetry. Top left: setup for single photograph capture using smartphone camera. Bottom left and right: setup for photogrammetry capture in overlapping photograph series, in several panoramic ranges, and at various angles and distances from the piece.

using the inverse vector transformation function in Grasshopper. To visualize the subsequently captured point clouds in Rhinoceros, a custom data recording module was created in C# [44] and implemented in Grasshopper. The captured point clouds were also saved as a .ply files to disk for further processing using a custom C# code [45], also deployed in Grasshopper.

## 2.2. Data processing

Stage two of the proposed process framework facilitates the processing of the captured data via filtering, clustering, and feature extraction. This stage relies on the prerequisite that the three different data formats generated in the first stage determine the specific, and differing, data processing routines. Thus, for 2D raster images, two tools are proposed that are well-suited for working with 2D image data: image-based ML algorithms pre-trained on large 2D image datasets, and CV methods for identification and extraction of characteristic features from raster images. For the first case, the open-source ML model Segment Anything [46], implemented in Grasshopper via CPython [47] and the Hops server add-in [48] was employed to generate the boundaries of characteristic wood knot features and other surface imperfections in the treated pieces. For the second case, to facilitate accurate identification of wood grain features and their representation as geometric objects, i.e., curves and lines, two CV methods from the open-source library OpenCV [49] were used, i.e., Canny Edge Detection, and Hough Line Transform. The implementation follows the workflow proposed in [16].

For the handling of object data in the point cloud format, custom computational routines were established. They were supported with two add-ins enabling point cloud processing within the Grasshopper environment, i.e., Cockroach [50] and Volvox [51]. Cockroach aided the process of clustering the points into groups based on a defined set of data embedded in the point cloud. This helped to identify and cluster those points within the point cloud that exhibited characteristic features of the physical pieces, namely similarly colored surface damages, chippings, and wood knots. Volvox helped in the filtering and culling of the point cloud by using clipping planes as well as assigning to each point extra data parameters computed from the raw point cloud data. For instance, average brightness values were calculated and assigned to each point,

based on the red, green and blue (RGB) color data values, and employed to filter out the points having brightness values within a given range.

For the processing and filtering of object data in a textured 3D mesh format acquired using photogrammetry, custom computational design routines within Rhinoceros 3D and Grasshopper were created. Upon import into Rhinoceros 3D, the meshes were pre-processed. They were rotated and aligned with the horizontal plane in the world coordinate system, scaled to match the physical dimensions of the pieces, and cleaned up by removing unnecessary geometric information. All these operations were done using standard transformation and mesh tools in Rhinoceros 3D. To access and extract the mesh data describing the surface fragments of the wooden pieces to be treated, Boolean operations in Grasshopper were deployed. The negatives and subsets of the objects could be generated and extracted, with direct access to their topological data provided by Grasshopper's standard Deconstruct Mesh method. In this way, the information describing the mesh faces, vertices, colors, and normal vectors could be filtered and sorted, ultimately serving as a basis to perform the geometric toolpath construction operations in the next stage of the process.

## 2.3. Data-driven generation of robotic fabrication sequences

Stage three of the generic process is dedicated to robotic 3D print path construction and generation, featuring various levels of automation. The paths, in the final form represented as points and curves, are generated via automated or semi-automated computational routines, or constructed through geometric routines. Both the generation and construction operations are always informed by the data extracted using the methods from the previous stage. Like in the previous stage, the prerequisite here is that the different character and scope of the extracted data determines, guides, and limits how this data can be utilized to create the 3D printing paths. In the experiments, six different methods for 3D print path generation were developed and demonstrated for three reuse scenarios: applying a revitalizing surface texturing, repair through new additions, and reassembly into new configurations.

The 3D printing path generation methods for new texture augmentation were driven by features extracted from 2D images using ML and CV. Because of the two-dimensional character of these data representations, the 3D print path designs were at the outset based and driven

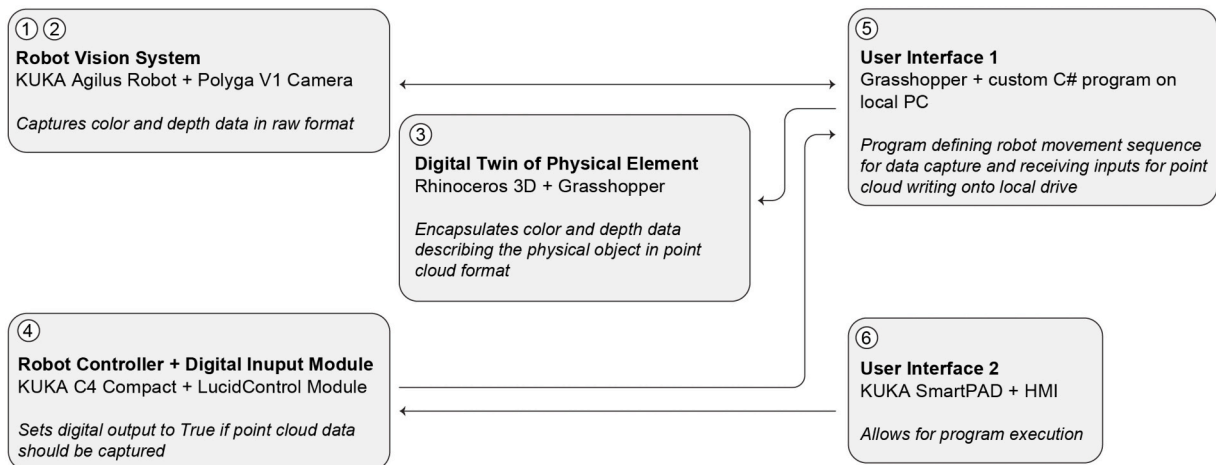
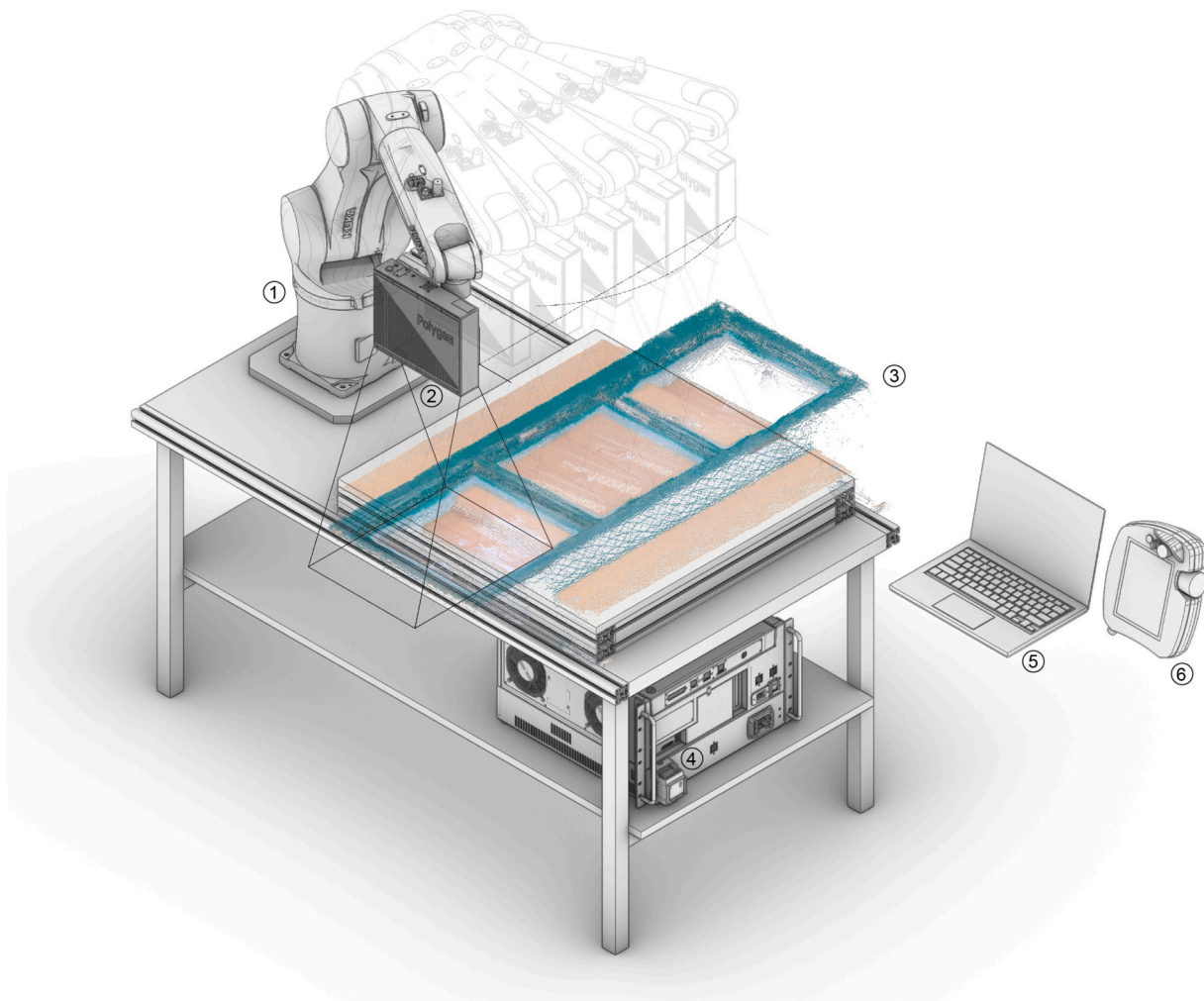


Fig. 4. Custom-developed robot vision system facilitating point cloud data capture.

only by these 2D features, represented as 2D curves, without any 3D data about the components' surface topology. The two path generation methods employed were: a custom-developed program based on a custom-developed differential growth algorithm [52], and iterative particle tracing in a vector field done using the Anemone add-in [53]. These two methods yielded planar 2D curve representations of the printing paths. To compensate for the lack of depth data and allow for the path fabrication onto three-dimensionally shaped surfaces of reclaimed components, an additional step of projection onto a mesh

geometry acquired via photogrammetry was employed. In this way, it was possible to create 3D representations of the paths that were aligned with and following the outlines of the surfaces onto which they would be applied.

Different routines were developed for the paths representing new textures generated using the points from the 3D point clouds. The first approach was to cluster the points based on the darkest color values and then generate the paths from clusters of points automatically using the Voronoi diagram method. The other method featured geometric

construction of custom line patterns, generated by grouping the points from the point cloud based on their brightness values, and then sorting and shifting them based on Cartesian coordinate values. Ultimately, however, because the resultant patterns were two-dimensional, an additional step of realignment with the point cloud was employed as support. The depth of the paths was adapted to the treated surface's outlines by assigning the z coordinate values of the points from the point cloud to the z values of the toolpath points, based on point proximity.

The 3D printing paths describing volumetric additions fitted to the existing components, and generated based on 3D data from the digital twin meshes, did not require projections or readjustments of the paths. This was possible because the digital data format of the mesh captures the 3D topological information about the objects. Thus, the paths could be created directly by using the geometric data of the mesh. Therefore, the fifth and sixth method of 3D print path generation focused on harnessing the geometry data acquired from the 3D meshes. Through custom computational design routines based on Boolean volume difference operations via the Dendro add-in [54] for Grasshopper, and voxelization as well as mesh sectioning using the standard Grasshopper methods, they allowed to create 3D printing paths that adapt to the unique boundaries of the reclaimed wooden pieces.

### 3. Results

The generic process described above was verified and implemented in six experiments, based on design and prototyping, and featuring custom workflows and toolkits combined in different ways throughout the generic process framework stages. The workflows utilize in diverse ways three types of data describing the treated components' features, i. e., 2D raster image, 3D point cloud, and 3D mesh. The overarching goal was to support versatile 3D print path design strategies for various types of component reuse interventions. The results and implications of each workflow are presented in more detail below, followed by a summative discussion of the findings.

#### 3.1. Digital workflows harnessing 2D raster image data

The two digital workflows supporting path generation presented herein relied on data extracted from raster images. The raster size corresponded to the output image resolution in pixels, set by the user for the digital camera employed to capture the images. As the data representation was in this case restricted to planar 2D data that the digital photographs provided, and the ML algorithms utilized in this

experiment were designed to handle only 2D image input [46], the path designs were also generated as 2D constructs. Due to this two-dimensionality, it was presumed that the best design application of this output would be 2D texturing patterns, printed onto the treated surfaces.

The first patterning workflow, verified in the first experiment and shown in Fig. 5, supported the design of a texture generated computationally using a differential growth algorithm informed by ML-extracted surface features. The process began with component digitalization by capturing it in a top-view photograph using a digital smartphone camera. The photograph was used as input for a pre-trained ML algorithm for image segmentation that returned the boundaries of characteristic features in the physical component, namely the outer boundary, and wood knot outlines. These features, represented as curves, were then employed as boundaries limiting and guiding the custom-developed differential growth algorithm that generated a continuous, closed polyline curve adapted to the input boundaries. In the final step, to facilitate robotic 3D printing onto the surface of the component, the curve was projected onto a digital twin mesh representing the component and acquired through photogrammetry. This ensured that the curve follows the surface outline upon fabrication. The resultant physical prototype with the regenerative pattern applied onto its surface is shown in Fig. 6.

The second workflow, presented in Fig. 7, featured a particle-traced path generation guided by the orientation and layout of wood grain features found using the CV methods specified earlier. As in the previous workflow, the element was first captured in a digital photograph. The photograph was then subjected to a series of computational data conversions involving the CV algorithms. To start with, the initially colored photograph was converted to a black and white image with increased contrast values. Then, the image was binarized based on a given threshold, and the Canny Edge Detection CV method was employed to extract the edges between the black and white areas. Thereupon, the Hough Line Transform OpenCV method was used to generate lines based on the pixel data describing these edges. The computed lines represented an approximated representation of the wood grain features in the original piece. Next, the wood knot features were also found within the image using the same ML method for image segmentation as in the previous experiment. In a subsequent step, the found lines and knots informed the generation of a vector field with forces following the grains and repulsing from the knots. A computational process of particle pathway tracing in this vector field, featuring collision avoidance between the particles and path adaptation to the found grain and knot

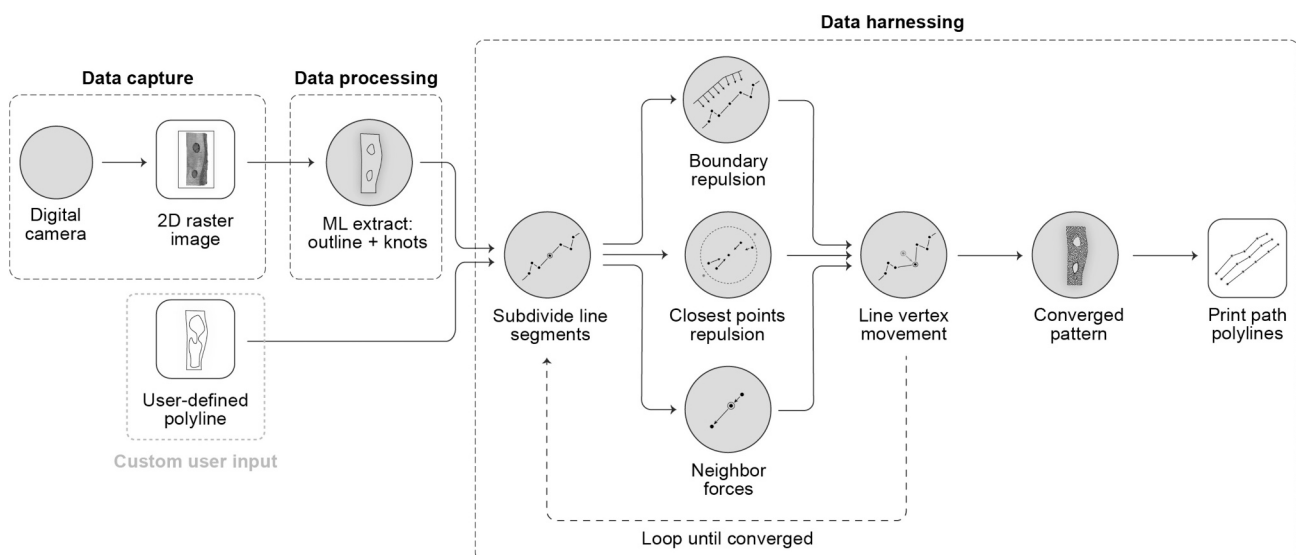


Fig. 5. Digital workflow in experiment one with feature-adaptive element texturing informed by ML-based feature extraction from 2D image data.



**Fig. 6.** Design outcome of experiment one, embracing two reclaimed wooden floorboards (top) decorated with new 3D printed textures (bottom left and right) generated using differential growth algorithm adapting to unique shapes and layouts of wood knots, cracks, and irregular outlines of treated pieces, found using ML.

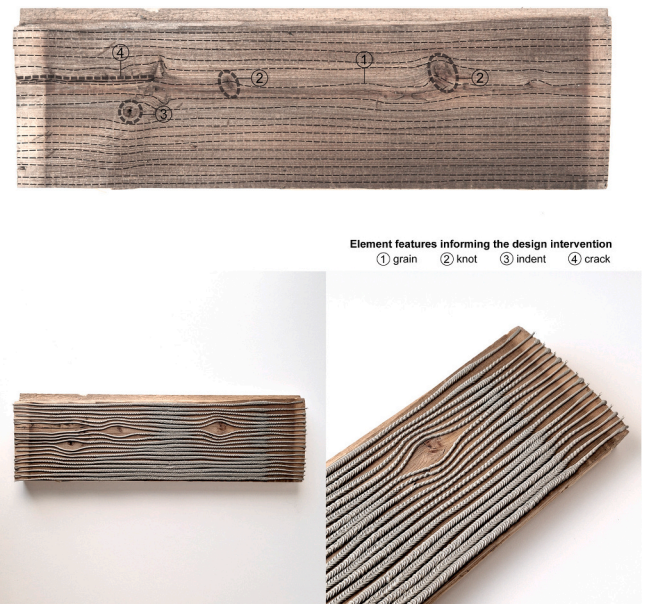
features, was then used to generate the paths. The traced paths were augmented with further data mediating intricate detailing, achieved by modulating the 3D printing speeds based on the distance to the features. In the final stage, the paths were projected onto a mesh, to ensure that they accurately follow the treated element's silhouette. The resultant prototype with a new texture is shown in Fig. 8.

Based on these experiments, it can be stated that the main advantage of working with 2D image data resides in the quick and simple capture of this data using commonly available tools, a smartphone, or a digital camera. Another advantage is the possibility of swift extraction of unique features of the treated component from its single image representation, using open-source pre-trained image segmentation ML

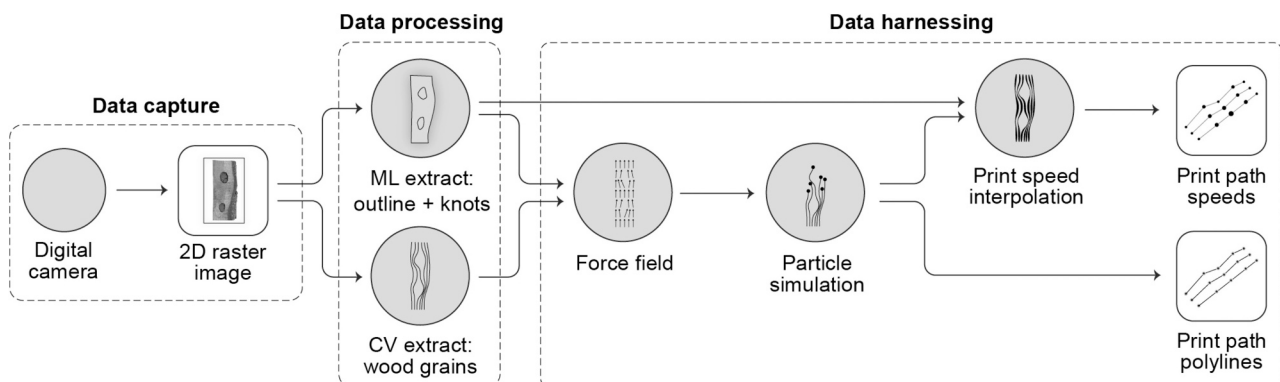
algorithms and established CV methods. Specifically, the employed ML algorithm, Segment Anything (SA), is a robust tool because it is pre-trained on a large dataset of 1 billion masks and 11 million images, which allows it to return valid segmentation outputs, given any segmentation prompt, in real-time [46]. The model is inspired by prompting techniques used in neural language processing (NLP) and computer vision that can perform zero-shot and few-shot learning for new datasets and tasks, which entails that either no or only a few labeled examples are needed for its training [55]. As such, the SA model is based on an image encoder that computes an image embedding based on an input image provided by the user, a prompt encoder that embeds user prompts defining what is to be segmented in the given image, and a mask decoder that combines the previous two information sources and predicts the segmentation masks within the input image [46].

Both experiments show that the features found using both the ML and CV methods can be easily harnessed to inform, limit, and drive the design expression of the reuse interventions adapted to designated features. This facilitates the creation of customized, element-specific textures that highlight unique features found in the treated elements.

The main limitation here results from the 2D character of input data from raster images. This 2D data does not provide the depth information



**Fig. 8.** Design outcome of experiment two, embracing reclaimed wooden floorboard (top) decorated with new 3D printed texture (bottom left and right) generated using custom particle tracing informed by unique wood grain and knot features found using ML and CV methods.



**Fig. 7.** Digital workflow in experiment two with feature-following element texturing driven by 2D image data extraction using ML and CV methods.



describing the topography of the treated surface, necessitating the use of a supplementary data source providing the missing depth information. In the experiments, this data was acquired via photogrammetry and a resultant 3D mesh representation. This mesh was utilized to project the 2D texture curves onto it, and therewith to add the depth data to the paths, ensuring that the 3D printer follows the element's surface.

### 3.2. Digital workflows harnessing 3D point cloud data

The two workflows presented here were devised to exemplify path generation based on 3D point cloud data capture. As the point cloud provides surface feature and depth information about the digitalized elements, it was deemed to be suitable for augmenting 3D printed interventions based on textural and volumetric surface indent patching and filling, as well as full-coverage repair interventions applied onto the treated elements.

The first patterning workflow, shown in Fig. 9, was informed by color and depth data from the 3D point cloud representing the treated piece. The design objective was to repair the local damages in the form of indents in the piece, by 3D printing a new material locally into the indents so that it fills them while also introducing a new texture around the patched-up zones. Firstly, the physical element was digitalized as a point cloud representation using the robot vision system. The point cloud was imported into Grasshopper. Then, the point cloud was filtered by normal values, brightness values, and location, to extract the points representing the indents within the treated piece. These filtered points were put into separate clusters based on mutual proximity. For each point cluster, an outer boundary curve was found using the Convex Hull method in Grasshopper. Each such boundary was then expanded and merged with the other boundaries. This merged polyline was utilized to trim the Voronoi cell diagram generated in the next process step. In that step, the point clusters were used as input for the Voronoi Diagram method in Grasshopper. The Voronoi cell sizes were fine tuned in the final step by iteratively recalculating the Voronoi Diagram using the looping function of the Anemone add-in. This resulted in a visually smoother gradation of the cell sizes, advancing from the centers of the defects towards.

The final Voronoi diagram represented a new material pattern for repairing the indents, where more material was featured within the indents through denser Voronoi cell packing, and the material volume decreasing further away owing to larger cells. Because the 2D Voronoi pattern did not provide the necessary connectivity and topology information about the captured surface, the final step was to realign the depth information for the points defining the pattern to match the depth information registered in a digital point cloud capture of the treated piece, acquired using the robot vision system. By assigning the Cartesian coordinate values for the depth to the pattern's points, the pattern was adapted to follow the treated element's outline. The resultant physical prototype is shown in Fig. 10.

The second patterning workflow, shown in Fig. 11, was informed by

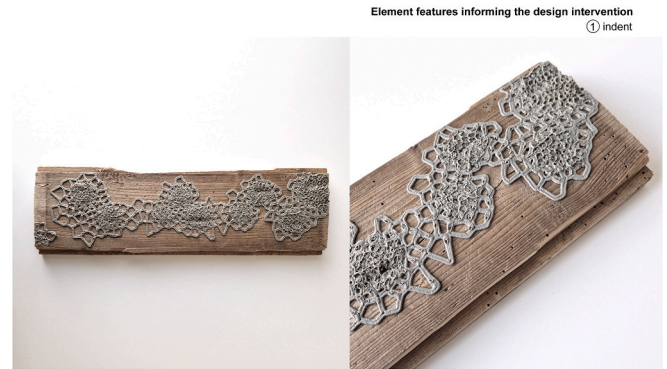


Fig. 10. Design outcome of experiment three, embracing reclaimed wooden floorboard (top) repaired by 3D printing material infills into indents (bottom left and right), with repair texture generated using Voronoi diagram construction informed by extracted point cloud data describing surface damages.

the RGB color values and Cartesian coordinate data from the point cloud representing the treated piece. The design objective was to apply a new finishing layer featuring full coverage with a new material, while highlighting the original discolorations of the covered surface through corresponding color variations in the finishing layer. Thus, after capturing the treated piece in a point cloud format, the Volvox add-in for Grasshopper was employed to cull that point cloud based on the brightness values calculated from an average of RGB color values of the points in the cloud. This resulted in two groups of points, i.e., the brightest and the darkest ones. For each group, the points were moved to follow a linear arrangement, which was achieved by reconstructing these points using new constant y-coordinate values for each linear row. Using these points as a basis, linear 3D print paths were constructed. For the remaining area of the surface that was neither the brightest nor the darkest but rather in-between, the linear paths were created by trimming a set of equally spaced line segments using the start and end points of the previous line groups, corresponding with the brightest and darkest zones. In the final step, the Cartesian coordinate values describing the depth of the paths were readjusted using the point cloud representation of the treated piece, as in the previous experiment. The final physical prototype is shown in Fig. 12.

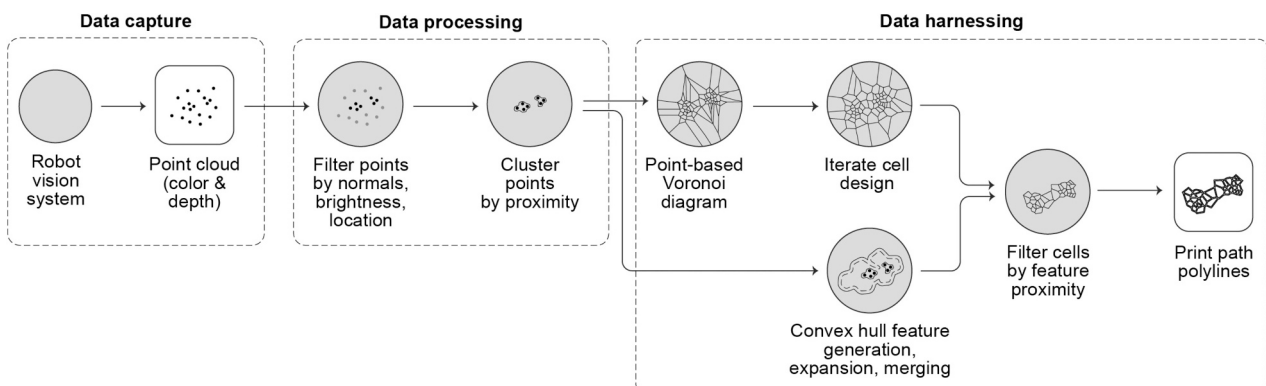


Fig. 9. Digital workflow in experiment three, with surface indent repair based on parametric feature extraction from 3D point cloud data.

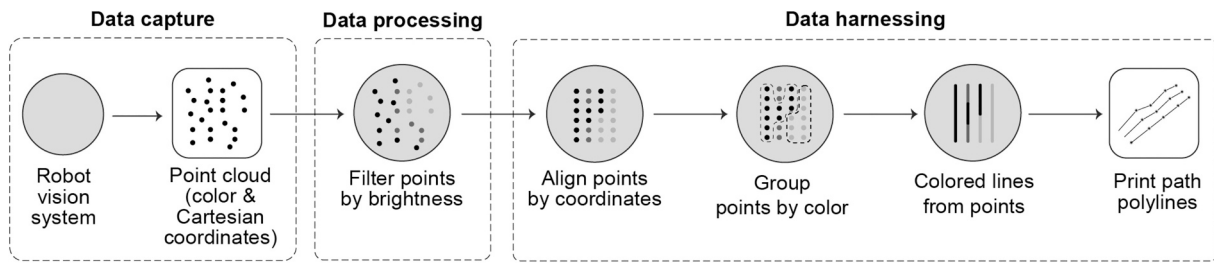


Fig. 11. Digital workflow in experiment four, with regenerative surface coating pattern created using parametric design informed by color and coordinate data from 3D point cloud.

As these two experiments indicate, the main advantage of working with the 3D point cloud data as a driver for the design of reuse interventions resides in the possibility of quick identification and extraction of the unique surface appearance features of the treated components from the cloud's embedded color and depth data. Specific points from the point cloud that correlate with the characteristic features of the reused components, such as chipped off fragments, cracks, or damaged coating areas, represented by points colored and positioned distinctively, can be identified, extracted, and clustered into groups. This, in turn, enables their use as guides for the machine toolpath design.

The main limitation here is the lower accuracy of color data representation in the point cloud compared to the 2D raster image. The two experiments have revealed that point cloud filtering based on color data outputs filtered colors that are highly approximated. Similar, non-contrasting colors, as well as the boundaries between the different colors, can be more difficult to identify precisely within the point cloud compared with the ease of their identification in a 2D image. Another potential limitation resides in the non-topological character of the 3D point cloud data, as it does not provide the point connectivity information and normal vector orientations of the points on the digitalized surface. Additionally, if the point cloud has insufficient resolution, there is a high risk of inaccuracy because the paths of the 3D printed

intervention may not always precisely follow the actual surface silhouette, in extreme cases mistakenly dipping into or protruding outside of it. Thus, volume-based reuse interventions in which full topology data is needed for the precise conduct of fabrication interventions, may not be feasible to carry out based on the point cloud information as the sole data source. The use of a supplementary data source, such as a 3D mesh, is needed in those cases, to provide the complete topology information.

The precision-related limitations of point cloud data could be mitigated using additional computational methods. One solution is to combine multiple data sources, following our proposal described above and in the earlier section of using an extra 3D mesh representation for toolpath projection, to ensure topological correctness of the 3D printing trajectory and precise alignment with the outline of the treated element. If numerical comparisons, using distance computation, of the offsets between point clouds acquired from various sources, or point clouds and meshes, are needed in the process of interpolating and approximating data from various sources, an open-source software CloudCompare could be used [56]. However, also other advanced multi-source data fusion methods, reported in prior papers, could be applied, such as those based on the fusion of point cloud and mesh data, yielding a 3D model that interpolates the data obtained from the two sources [57].

In the case when multiple point clouds need to be aligned and cleaned up, a possible solution is to employ advanced filtering techniques, based on the processing of RGB and depth data [58], image processing and point coordinate histograms [59], and deep learning methods [60]. These techniques help to, among others, remove noise and outliers, detect planar surfaces, eliminate unwanted elements, fill gaps in point clouds, and precisely extract characteristic spatial features.

### 3.3. Digital workflows harnessing 3D mesh data

In these two last experiments, the 3D printing of supplemental volumes instead of using subtractive manufacturing methods, such as milling, cutting or trimming the pieces, was chosen for three reasons related to the circular design aspects advocated in this paper. Firstly, the ambition was to use a fabrication method that does not introduce cut-off waste in the treatment process, which would have been the case if the elements were milled or cut into standard rectangular shapes. Secondly, the edges of the reclaimed pieces were irregularly shaped, making it difficult to achieve a perfect fit with other elements if techniques such as robotic cutting were used. Thirdly, 3D printing made it possible to design the added elements as non-solid ones, and thus use less material. Consequently, the 3D printing as a fabrication method of choice ensured a resource-efficient process, where the added elements were lightweight, manufactured with no scrap, and having edges precisely matching the outlines of the reclaimed wooden boards, without the need for material removal to achieve a good fit.

To further highlight the sustainability potentials of the proposed approach, the materials chosen for the additions encompassed bio-based composites containing hemp and wood fibers. This was meant to demonstrate the use of sustainable materials in the treatment process. Although the materials used here have not been studied from the



Fig. 12. Design outcome of experiment four, embracing reclaimed wooden floorboard (top) with new coating that approximates, through coloring variations, discolorations of piece underneath (bottom left and right). Texture generated using parametric construction methods informed by color data registered for treated piece via robot vision and extracted using 3D point cloud data filtering.

standpoint of applications in repair, their mechanical properties reported in the literature indicate good strength and stability for non-structural applications [61,62]. Thus, these materials were deemed viable for the non-loadbearing application demonstrated herein. Nonetheless, further research, beyond the scope of this paper, is needed to confirm this assumption.

The 3D printed additions can be connected to the original wooden floorboard piece in various ways. For instance, by using a system of metal anchors or rods added discretely at the back, or by using biobased adhesives [63]. Alternatively, assuming that the pieces would eventually be mounted as add-on cladding onto walls or ceilings, they could be attached to the main loadbearing system by screwing or via bespoke joinery features designed within the 3D printed elements.

The final two workflows relied on the data of a digital twin mesh model representing the treated piece, acquired via photogrammetry. As full 3D data was provided by this representation, the workflows were deemed suitable for applying volumetric additions and rearranging the reclaimed components into new configurations, using combinations of reused and newly fabricated materials.

The first workflow, shown in Fig. 13, was informed by the mesh surface and volume information. The design intention was to complement a material piece having two broken-off and irregularly shaped edges with two new volumetric additions, to bring the dimensions and edges of the damaged piece to a more regular and standardized form. The treated piece was digitalized using photogrammetry to obtain a digital twin representation as a 3D mesh. In relation to this mesh, a user-defined mesh volume was created, defining an approximated outline of a new spatial structure complementing the digitalized piece along its damaged edge. Both meshes were converted into volume representations via the Grasshopper Dendro add-in based on the OpenVDB library, to facilitate fast Boolean difference operations that allowed for the extraction of exact shapes that fit together with the original piece. The resultant volumes, representing additions to the existing broken piece, were then voxelized, and the voxels were augmented with a user-defined curve, inscribed into each voxel. To follow the irregular boundaries of the element, the curves inscribed into the voxels were additionally trimmed using the volumes generated in the previous step. The collection of these curves represented the 3D printing sequences for a spatial lattice structure of the addition, with one side perfectly matching the edge of the board to which it was to be docked, and the other following a straight line. The final physical prototype is shown in Fig. 14.

The second workflow, shown in Fig. 15, was also informed by the mesh data, in this case the data describing the surface outlines. Here, the design intention was to connect two physical components using a volume that fits between them. In the first process step, the components were digitalized using photogrammetry to obtain digital twin mesh models of the treated elements. A user-defined mesh was also created between these two meshes. All three meshes were then converted into volume representations via the Grasshopper Dendro add-in. An in-between volume was generated by calculating the Boolean difference between the user-defined mesh and the two meshes representing the wooden pieces, to derive a volume that accurately follows the inner, uniquely shaped edges of the pieces. This volume was then intersected with a series of equally spaced horizontal planes, yielding a series of

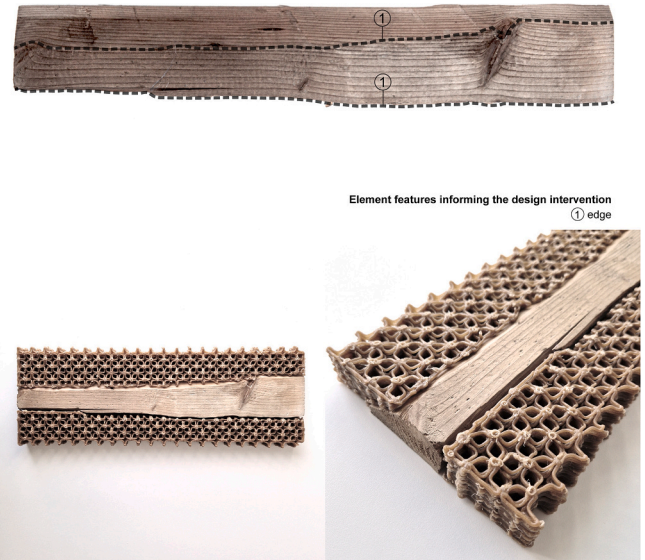


Fig. 14. Design outcome of experiment five, embracing reclaimed wooden floorboard (left) with irregular form brought back to standard form by adding two 3D printed supplementary volumes with straight outer edges and specified dimensions (middle and right). 3D print paths for additions generated through volume voxelization informed by geometric surface data describing broken-off silhouettes of treated piece and found using Boolean volume extraction.

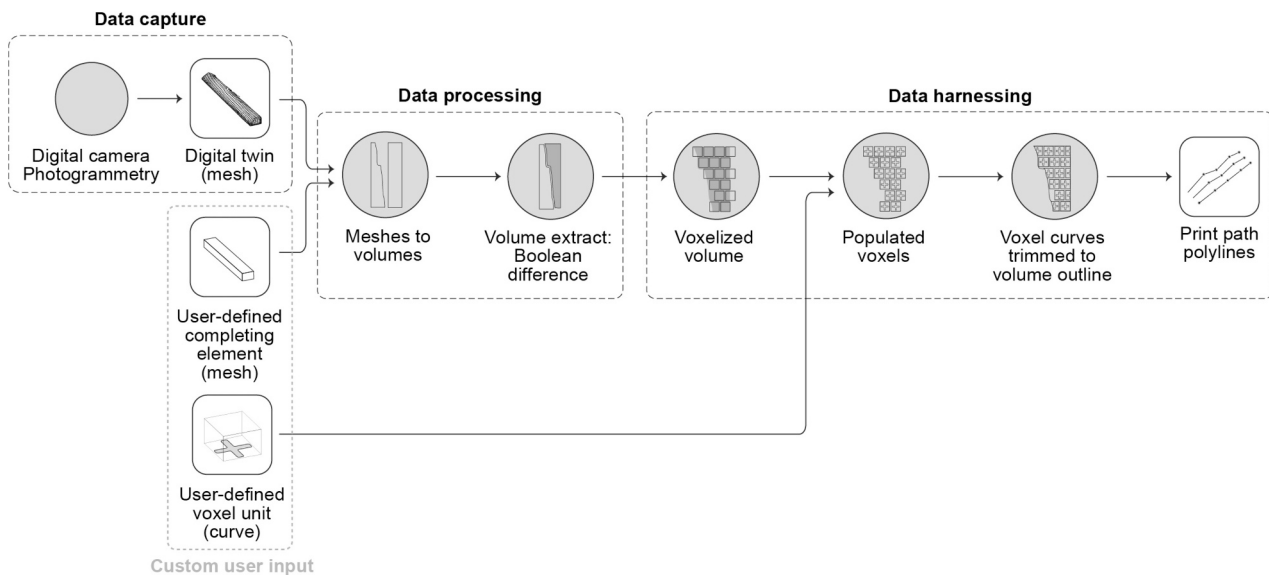


Fig. 13. Digital workflow in experiment five, with element repair through volumetric additions informed by unique spatial features acquired from digital twin 3D mesh data captured via photogrammetry.

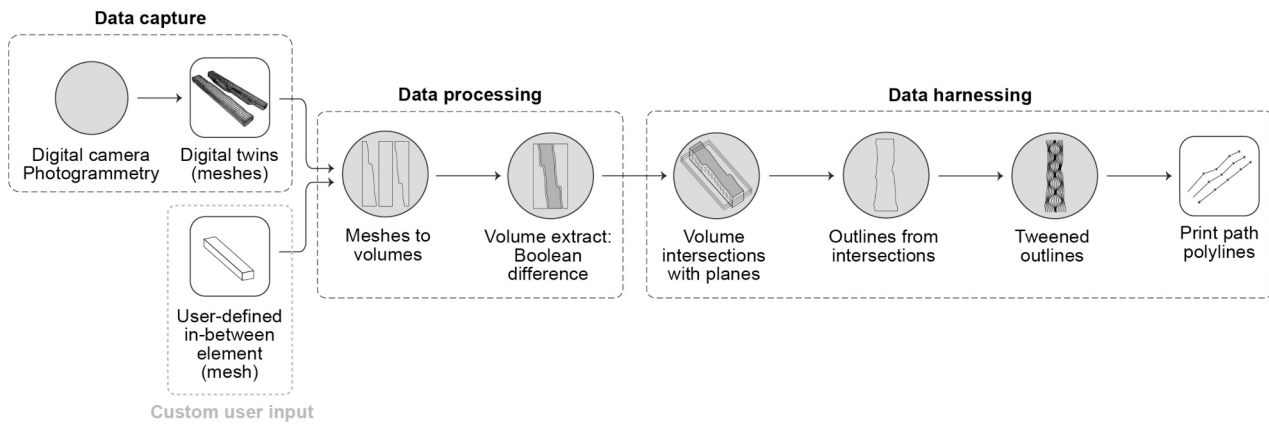


Fig. 15. Digital workflow in experiment six, with element assembly using custom interconnection piece informed by 3D surface and volume data extracted from photogrammetry-derived digital twin mesh model.

polyline curves. By computing the vector dot product between the tangents of each polyline's control points and a vector representing a Cartesian axis direction following the wooden elements' length, the curve fragments following the longer edges could be extracted as pairs of opposite curves. Between these curves, intermediate curves were created using the Tween method of the Pufferfish add-in [64] for Grasshopper. For these curves, the control points were shifted to the left or right of the main curve, to construct wave-like base curves. By generating additional intermediate curves between the edge and the base curves using the Tween method, the final paths were created. Fig. 16 shows the physical prototype manufactured using the described workflow.

The conducted experiments reveal that the main advantage of using

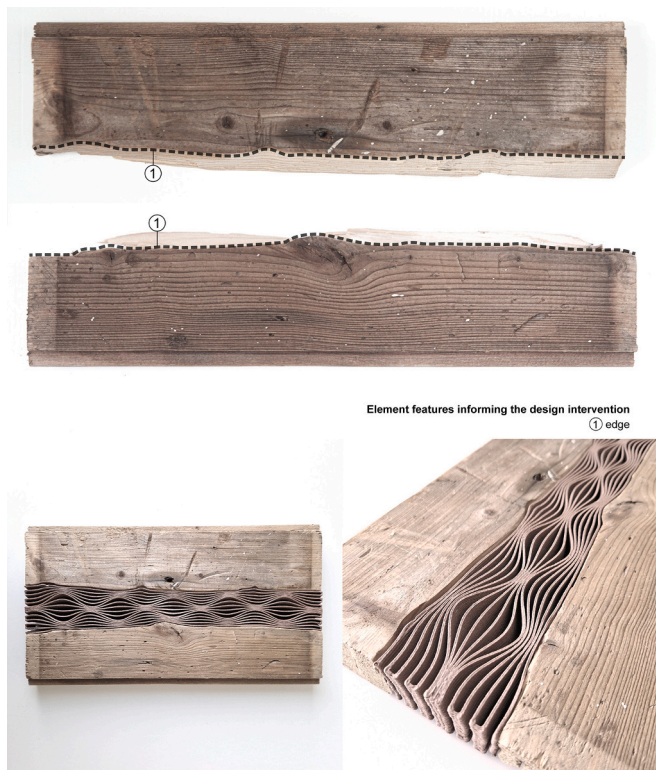


Fig. 16. Design outcome of experiment six, embracing two reclaimed wooden floorboards (left) assembled using new 3D printed interconnection piece (middle and right) designed using tween curve method informed by photogrammetry-derived mesh sectioning data.

the digital twin 3D mesh representations resides in the possibility of directly accessing the surface topology information. Once this information is available, the reuse interventions can be adapted to the unique surface outlines volumetrically, in all three dimensions. As the mesh representation conveys the spatial information about the element, it can be employed to drive operations on volumes, such as voxelization, Boolean operations, and slicing. The mesh information describes the treated objects fully, eliminating the need for engaging complementary data sources in the design process.

The main limitation concerns the difficulty in the filtering of the characteristic surface detailing features embedded in the components, such as knots, wood grains, surface chippings and damages. As the mesh representation captures the surface holistically, it is less suitable for extracting smaller and higher-resolution features in a workable way. The mesh texture provided with photogrammetry can be used but to a limited extent as the mesh faces to which the texture is mapped and projected have their restricted shape, such as triangles or quads, which can be more difficult to work with in relation to the often curved and intricate outlines of the features. Further, to access the discrete information describing its face vertex coordinates, colors and normal vectors, the mesh needs to be deconstructed. After the filtering and clustering of this deconstructed mesh data, it is difficult to return to a mesh representation. Thus, the mesh representation overall is suitable for interventions that primarily require access to surface topology information, in the cases where such information is needed to drive volumetric operations on the treated pieces rather than working with surface details and coloring.

#### 4. Discussion

A summative comparison between the prerequisites and outcomes of the conducted experiments is presented in Fig. 17. Overall, the experiments confirm that the digital process framework and the tooling ecosystem proposed in this paper support the fundamental steps needed to implement architectural reuse interventions involving reclaimed elements with unique, irregular features. The three main stages in the workflow, i.e. data capture, extraction, and harnessing, offer various options for data handling. The experiments showcase the robustness and broad possibilities of harnessing this data for design and manufacturing purposes. The three data capture methods provide different types and scopes of information about component geometry and unique appearance features, in diverse formats and at diverse resolutions, from the global geometry to localized and component-specific surface features at a magnified level of detailing. This presents potential for various areas of application, from the renovation and reuse of common, reclaimed architectural components and construction materials, to highly tailored treatment of elements having specific artistic, historic, or visual values,























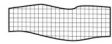



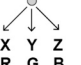
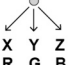
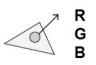
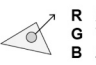






	Experiment 1	Experiment 2	Experiment 3	Experiment 4	Experiment 5	Experiment 6
<b>Treated features</b>	Wood knots Element boundary 	Wood knots Wood grains Element boundary 	Surface indents 	Surface discolorations 	Broken edges (inner + outer) 	Broken edges (inner) 
<b>Reuse application</b>	Embellishment [ Surface pattern ] 	Embellishment [ Surface pattern ] 	Repair + embellishment [ Surface infill + pattern ] 	Repair + embellishment [ Surface coating + pattern ] 	Assembly + repair [ Volume additions ] 	Assembly + repair [ Volume interconnection ] 
<b>Data capture tool</b>	Smartphone camera [ iPhone 11 ] 	Smartphone camera [ iPhone 11 ] 	Structured light robot vision camera [ Polyga V1 ] 	Structured light robot vision camera [ Polyga V1 ] 	Smartphone camera + photogrammetry [ iPhone 11 + KIRI Engine ] 	Smartphone camera + photogrammetry [ iPhone 11 + KIRI Engine ] 
<b>Input data</b>	Raster image [ 2D ] 	Raster image [ 2D ] 	Point cloud [ 3D ] 	Point cloud [ 3D ] 	Mesh [ 3D ] 	Mesh [ 3D ] 
<b>Data type advantages</b>	Color information [ RGB values ] 	Color information [ RGB values ] 	Color + depth information [ RGB values + Cartesian coordinates ] 	Color + depth information [ RGB values + Cartesian coordinates ] 	Color + depth + topology information [ RGB values + Cartesian coordinates + normals ] 	Color + depth + topology information [ RGB values + Cartesian coordinates + normals ] 
<b>Data type limitations</b>	No depth information	No depth information	No topology information	No topology information	Limited color information	Limited color information
<b>Feature extraction method</b>	Machine learning [ Segment Anything Model ]	Machine learning + computer vision [ Segment Anything Model + Open CV ]	Point cloud filtering [ Volvox + Cockroach ]	Point cloud filtering [ Volvox + Cockroach ]	Mesh to volume + voxelization [ OpenVDB/Dendro + Grasshopper ]	Mesh to volume + sectioning [ OpenVDB/Dendro + Grasshopper ]
<b>3D print path generation method</b>	Semi-automated [ Custom differential growth algorithm + user input ]	Automated [ Particles in force field simulation ]	Automated [ Voronoi diagram ]	Automated [ Grasshopper ]	Semi-automated [ Volume extraction and voxelization + user input ]	Semi-automated [ Volume extraction and sectioning + user input ]
<b>3D print path geometry</b>	Closed polyline [ Single continuous curve ] 	NURBS curves [ Planar group ] 	Closed polylines [ Multicellular arrangement ] 	Line segments [ Planar-like groups ] 	NURBS curves [ Spatial lattice ] 	NURBS curves [ Planar groups arranged spatially ] 
<b>Path generation time</b>	Minutes to hours	Minutes to hours	Minutes	Seconds	Seconds	Seconds

Fig. 17. Summative comparison between prerequisites and outcomes of six prototyping experiments.

relevant in contexts such as architectural restoration and preservation.

Because each data capture method is limited in the type of information about the component features it provides, combined use of several methods is to be expected, to seize the strengths of each method and mitigate its deficiencies. The six workflows based on the generic process framework show that the proposed tooling ecosystem can be combined into various tool combinations and applied for various architectural reuse cases: from new surface finishes and decorative texturing treatments, through damaged component repair, up to creating new spatial arrangements of uniquely shaped and custom-sized reclaimed elements, regardless of how intricate each of them is. Holistic data describing the components can be acquired using a combination of

methods, and then arranged, sorted, and filtered in diverse ways, to ultimately inform and drive the generation of robotic fabrication sequences, contributing to the potential of the proposed solution to effectively support the architectural process of reuse, from design to production.

To forecast the suitability of the proposed framework for large-scale applications in practice, the key aspects relating to the scaling up, economic feasibility, and environmental benefits are discussed below, using references from already published papers as support.

#### 4.1. Framework applicability in real-world construction projects

In this section, the challenges of applying the proposed framework in practice are identified and some solutions to address these challenges are proposed. Two probable application scenarios are discussed, i.e., component reuse, and component renovation or restoration.

In an architectural scenario featuring component reuse, the first challenge is to identify suitable, locally available materials. To facilitate this, digital databases of such materials, in the form of public online cadasters and catalogs, are being continuously developed [65,66]. Importantly, however, the material and component data in these repositories is limited to suit the purpose of conveying the basic information, such as material and component typology, general condition, available quantity, and global dimensions [7]. Thus, although this generic data helps to identify materials suitable for purchase, it is insufficient for the next stage of the process, i.e., design with reused materials. If components are sourced directly at the site, the issue of digitizing them also remains. Consequently, precise data registration on a component-to-component basis is required to capture all relevant geometric features, damages, degraded parts, and textural characteristics, and this is where the utility of the first part of our framework, focusing on detailed data capture, emerges. The choice of these detailed data capture techniques will depend on the project brief, existing user access to software and hardware, and the specifics of the location where digitization is to take place. Thus, two further options are considered here, for digitization but also treatment application—on-site and off-site.

The on-site option is probable in a historic building where renovation, restoration or preservation is to be done, and where materials and elements cannot or should not be dismantled. This option could also be relevant in projects where it is preferred to dismantle and treat elements directly on-site. In these instances, spatial access allowing to conduct precise scanning is required. An immediate challenge here is that some elements might not be within easy reach due to placement or dimensions. If this is the case, the data capture instruments proposed in the framework can be replaced with other hardware. For example, at sites featuring limited access or small spaces, where photographing for photogrammetry cannot be easily done, handheld scanners present a viable alternative [67]. If external parts of a building or a large interior space are in question, using drone-based, close-range aerial photogrammetry could be a feasible solution [68,69]. For especially large elements, mobile robot platforms equipped with robot vision systems could also be used for stepwise scanning [70,71].

For the on-site applications described above, a similar accessibility challenge concerns the 3D printing and other fabrication interventions at difficult-to-reach locations. If robotic arms and mobile robot platforms cannot be used due to limited access and the need for extended reach, an alternative is to deploy a distributed 3D printing system based on collective robotic construction (CRC) principles [72]. For instance, a mini mobile robot swarm, or an autonomous drone swarm that deposits the material locally [73,74]. For printing on existing tilted or vertical surfaces that are impossible or not intended to be demounted, robotic 3D printing using materials and end-effectors engineered for non-horizontal deposition, as well as spray-based 3D printing could be applied [75,76].

The second scenario, encompassing off-site fabrication, is probable for commonplace reuse and adaptation projects involving residential and commercial buildings. In that case, the elements purchased at the reuse marketplace could be digitized off-site, using the techniques from the framework, or a set of alternative hardware solutions described above for the on-site scenario. Then, the challenge of conducting the fabrication interventions needs to be tackled. One solution, is to deploy the interventions on-site, using the means described in the paragraph above. Another alternative, relevant to consider due to the digitization shifts of the architecture and construction sector toward Industry 4.0 solutions and new business models [77], is that components are delivered to a specialized robotic repair and renovation facility to undergo

reparative treatment. Thereafter, they could be transported to the site and built in directly.

In such a robotic repair and renovation facility, specialized robot teams can be deployed, executing tailored tasks that fulfill the specific needs of reuse and renovation treatments. The robot team would then have to be installed as part of a specialized, automated production line, which, in a basic setup, would feature a station equipped with robot vision systems for recognizing, inspecting, digitally registering, and 3D scanning the incoming elements, a 3D printing station for element repair and embellishment, and a quick-response (QR) code application station facilitating element labeling for later identification in the parametric 3D model or a BIM model as well as on-site. Optionally, also a milling and cutting station for joinery manufacturing and trimming to size, and possibly also an assembly station if the components would need to be pre-mounted before transportation to the site. Examples of such specialized robot cells and robot teams were proposed in prior research within architectural robotic fabrication [22,78–81]. The manufacturing automation research also offers important knowledge on the design of robot cells that are rapidly reconfigurable, and feature flexible tool exchangers, vision systems, as well as external robot axes comprising rotary tables and rails that allow for robust element positioning and processing [82]. Thus, because of the wide array of industrial robot customization options, such as adding extra cyber-physical sensing systems for real-time material monitoring [83], and a virtually limitless range of end-effectors that can be tailored for different fabrication processes [84], it is reasonable to assume that such a robotic repair and renovation facility could not only be successfully deployed but also reconfigured over time, to adapt it to ongoing renovation and reuse market demands and specificity of the handled materials.

#### 4.2. Economic feasibility of the proposed digital tool integration in architectural practice

Any project involving reuse, renovation, restoration, or preservation will be unique due to the individualized character of reclaimed materials and architectural settings. Further, the project portfolios of architectural offices differ, ranging from very specialized to very diversified. Thus, the potential return on digital technology investments needs to be considered at an individual level and in the case of diverse and fluctuating client portfolios may be difficult to generalize. However, there is research evidence suggesting that digitization in general is economically motivated in projects where circular design strategies, such as reuse and renovation, are applied [85,86]. It was also suggested that for short-term projects, equipment rental is most feasible economically, whereas an investment in precise scanning equipment is financially motivated in a long-term perspective [87]. Thus, the former applies if the reuse and preservation projects are commissioned rarely, whereas the latter applies in cases where such projects occur frequently. Further, there is also an option of utilizing a growing number of low-cost and open-source scanning solutions, feasible in cases where less precise results are acceptable [88,89]. Such solutions could be applicable to projects where large numbers of similar and non-complex components or materials, such as common windows, doors, structural elements, and bricks, are salvaged and reused.

To obtain a cost estimate for implementing the proposed framework, a compilation of software and hardware expenses is presented in Table 1, for two scenarios. The first scenario is based on new purchases only and thus entails larger costs. This scenario was implemented in this paper. For comparative purposes, a second, lower-cost scenario is also presented, in which some of the listed products are bought as second-hand merchandise. The costs of using the CV libraries and ML models are not included in any of these two calculations, as these tools are to date open source.

As seen from this estimate, the largest costs concern the scanning equipment and the industrial robot. However, if used products are purchased, the costs can be lowered by at least 60 %. The exact saving

**Table 1**  
Investment cost estimate for framework proposal implementation, for new and used products.

Software or hardware type	Commercial name	New product price [USD]	Used product price [USD]
Digital camera (smartphone)	iPhone 11	500	250
Photogrammetry software	KIRI Engine app (open source)	0	0
Robot vision system (structured light camera)	Polyga V1	12,000	8500 <sup>a</sup>
Mesh and point cloud management software for camera	FlexScan3D (included in the scanner price)	0	0
3D modeling and computational design software	Rhinoceros 3D with Grasshopper (commercial version)	1100	1100 <sup>b</sup>
Robot programming software	KUKA prc (community version)	450	450 <sup>b</sup>
Extruder for 3D printing and microcontroller system	E3D Titan Aero	150	150 <sup>b</sup>
	Ramps Shield	20	20 <sup>b</sup>
	Arduino Mega	30	30 <sup>b</sup>
Industrial robot including system software	KUKA KR10 sixx R1100	50,000	15,000
<b>Total cost</b>		<b>64,250</b>	<b>25,500</b>

<sup>a</sup> 3D scanner Artec Eva with comparable parameters, price source: [ebay.com](https://www.ebay.com), queried on Aug 20, 2024.

<sup>b</sup> Purchase of used product not applicable due to non-transferrable software license or already low price for new product.

capacity will depend on the availability of items with lower prices on the second-hand market. If buying used products is not viable, an alternative is to outsource the scanning and fabrication tasks to specialized companies, or to an academic institution with digital scanning equipment and a robotic fabrication lab. The feasibility of the first option is confirmed by the fact that such companies already exist on the market. For instance, the Spanish interdisciplinary studio Factum Arte offers advanced scanning and historic reproduction services [90], the Swiss company Design-to-Production [91] provides services bridging the design, fabrication, and construction stages in complex projects, and the Finnish Hyperion Robotics startup offers sustainable, large-scale robotic 3D printing services [92]. Successful cases of industry-academia collaborations also exist. A recent example is the demonstrator project DFAB HOUSE in Switzerland, where scholars from the Swiss National Centre of Competence in Research (NCCR) collaborated with 40 industry partners to digitally design and construct a fully operational, code-compliant building [93].

Simultaneously, a scenario based on an in-house use of robots and other fabrication machines within architectural offices or construction companies is also relevant to consider due to the evolving business models and new specialist roles in Architecture, Engineering, and Construction (AEC), related to automation and digitalization [94–96], as well as the success of already reported endeavors. To exemplify, the architectural office Rael San Fratello from the USA developed accessible, mobile digital fabrication platforms for large-scale 3D printing with local materials and employed them in construction projects [97].

Overall, the promising economic prerequisites outlined above, the emerging new services in the construction business, and a growing number of successful use cases point at the topicality of the proposed framework and give a good prognosis for its wider adoption in the AEC sector.

#### 4.3. Environmental benefits of robotic 3D printing and reuse supported by the framework

The sustainability of 3D printing as a product manufacturing

technique is already well established due to its waste-free mode of production and decrease in scrap material [98]. The general environmental impact of 3D printing is claimed to be up to 70 % lower than for other manufacturing techniques [99]. Owing to these promising indications, the sustainability of robotic 3D printing was also investigated in architecture and construction. Specifically, life cycle assessment (LCA) analyses were carried out to establish its environmental impacts and determine the most optimal application contexts. Interestingly, the main potentials of lowering the environmental impact of construction through robotic 3D printing were identified not in the typical manufacturing parameters, namely material use, and energy expenditures. Rather, in sustainable material solutions this technique allows to implement [100]. It was discovered that 3D printing can reduce the bulk of environmentally impactful, highly industrialized building materials and standardized components at the construction site by facilitating the production of custom, highly optimized structural elements from functionally graded materials, tailored to minimize waste generation, emissions, and resource consumption [101]. A comparative LCA analysis between non-standard robotic additive construction and construction using standardized prefabricated components indicated a 50 % lower total environmental impact and 45 % reduction in carbon dioxide emissions for robotic 3D printing [102]. Prior papers also suggested that the most justified and environmentally profitable application of robotic 3D printing is in the production of building components with non-standard, geometrically complex features [103]. For such components, when this technique is applied, it can lower the material usage and decrease carbon dioxide emissions by 33 % compared with a conventionally designed and traditionally built structure, and the environmental impact does not increase with an increase in geometric complexity [104]. Further, the robotic 3D printing technique was also shown to be most economically viable for low-volume production, yielding freedom in design and a building rate of produced square meters per hour 40 % higher compared with traditional construction on-site [105].

Overall, these prior findings lead to an inference that the applications of robotic 3D printing proposed in this paper, i.e., in the renovation and repair of uniquely shaped reclaimed building materials, and in the restoration or preservation of elements with non-standard dimensions and architectural features, are well justified from the environmental perspective. Many reused components available on the salvaged materials market will have structural and textural flaws as they may have been damaged upon demolition and demounting, and additionally originate from different buildings and thus have various shapes and dimensions. Their regenerative treatment via custom robotic 3D printing interventions can ensure that they are successfully repaired and accommodated in new architectural contexts. Also, in the historic conservation and restoration contexts, where low-volume, one-off custom production is typical, the technique can be applied as a sustainable alternative that allows for the elimination of time-consuming and human labor-intensive tasks involving manual application of materials onto the treated surfaces.

Regarding the environmental benefits of building material reuse generally, and timber specifically, LCA analyses suggest positive effects compared with new construction and reuse of other materials. It is already confirmed that recycling and reuse of materials in construction can lower greenhouse gas emissions by 37 % [106]. Further, the reuse of materials, and specifically the cascading of construction timber, targeted in our paper, can profoundly decrease the environmental impact of construction [107]. Timber as a construction material has great carbon storage capacities and for this reason is considered as one of the most sustainable building materials among the mainstream ones, dramatically outperforming steel and concrete. To illustrate, the global warming potential (GWP) of concrete is 273 kg CO<sub>2</sub>-eq, whereas for timber the value is negative, i.e., –656 kg CO<sub>2</sub>-eq [108]. Further, timber already present in existing buildings absorbs 582 kg of CO<sub>2</sub>, while reinforced concrete emits 458 kg CO<sub>2</sub>/m<sup>3</sup> and steel 12.087 kg CO<sub>2</sub>/m<sup>3</sup> [109]. On

top of this, LCAs indicate 53–75 % reductions across six different environmental impact categories for renovation compared to new construction [110].

Overall, these findings suggest that the life-prolonging strategies for reclaimed timber, including the renovation and repair of non-standard timber elements enabled via robotic 3D printing as proposed in this paper, are justified and beneficial from the sustainability perspective. As such, they can further lower the impact of construction on the natural environment.

#### 4.4. Comparative analysis of the proposed framework with current methods of material reuse

The reuse projects reported in the current literature rely on two main strategies for accommodating reclaimed materials and components. The first strategy is to use elements as they are and with minimal intervention to their form and surface finishing, which usually entails only cleaning and optionally also painting [111]. If reclaimed materials are uniform, traditional construction techniques can be used and no prior digitization of the materials is needed, with elements assembled and adaptations made on-site or off-site, using manual labor [112]. Alternatively, if the reclaimed components are more heterogeneous, a combination of digital and manual methods is used, starting with 3D scanning and 3D modeling, to digitize and design with reclaimed materials, followed by on-site joinery and assembly of the actual components by skilled human labor [113].

On the other side of the spectrum are reuse projects in which the salvaged materials are significantly altered, to adapt them to standardized dimensions and common formats [111]. In these approaches, assembly optimization using parametric and computational techniques [3,114], followed by robotic milling or cutting to fabricate precise connections and fittings is often employed [6]. In simpler projects, these interventions can also be done using traditional techniques at the construction site, such as saw cutting by workers.

Overall, the main drawback of these two approaches is that they introduce significant design limitations. Specifically, they limit the current reuse and renovation practice to either utilizing the materials and components as they are, with restricted possibility to redesign their aesthetic appearance, or the need to radically alter the dimensions and form of the elements by cutting, milling, and reassembly, to standardize them. Thus, both strategies limit the architectural design possibilities as well as the ranges and quantities of materials and components that will qualify for reuse given the applied restrictions. If cutting, milling and sawing are employed, an additional drawback is waste generation. In cases where manual labor and traditional techniques are used, the issues of inaccuracy of these processes can also contribute to waste generation and limit the architectural diversity and the on-site assembly options to those that are executable by human workers.

Compared to traditional practices, the advantages of the framework proposed in this paper are the increase in design freedom and the seamless transitions from element digitization, through redesign, up to the fabrication of the intervention. The immediate challenges of implementing the framework relate to the sophisticated digital skillset needed to use it, as well as the potential limited access to high-precision equipment in more demanding projects where advanced digitization methods and renovation techniques will be required, for instance in historic buildings. Nevertheless, the already mentioned transitions observable within the construction industry [77,94–96] as well as the advances in architectural education, concerning the growing number of courses and curricula in advanced computational design and robotic fabrication [115–117], promise to mitigate these challenges within a short time frame.

## 5. Conclusions

This paper puts forth a generic digital process framework and six

proof of concept workflows, aimed to support architectural reuse. The framework and workflows feature integrations of six advanced digital tools, i.e. photogrammetry, robot vision, machine learning, computer vision, computational design, and robotic 3D printing. As such, the established framework and its application examples provide the currently missing knowledge concerning such integrations, with architectural reuse as the targeted area of application. The prototyping experiments utilizing the workflows offer deeper insight on the advantages and limitations of different data sources in driving the design process toward fabrication.

Overall, the results of the experiments show that: 1) a digital tooling ecosystem comprising the six integrated tools provides an effective platform for supporting the design and execution of diverse architectural reuse interventions involving damaged components and uniquely shaped reclaimed materials; 2) different scenarios for combining the tools in the ecosystem are possible to devise to effectively support the redesign and robotic 3D printing, therewith supporting various architectural scenarios of reuse where existing and new building materials are combined into hybrid material systems; 3) digital data capture describing the unique features of reclaimed architectural components, in various formats, can be successfully harnessed to inform and drive the generation of machine path designs and robotic fabrication sequences; 4) the proposed integration supports a complete reuse workflow and all its stages, i.e., capture of data describing the salvaged components, redesign, and fabrication of the reuse interventions.

These findings contribute to the advancement of digitally aided reuse practices in the construction sector, offering novel insight on how to accommodate highly heterogeneous reclaimed materials by seizing the potential of advanced automation and digitization. The paper discusses and demonstrates how advanced tools can be integrated into the design-to-production chain and facilitate salvaged component repair and reuse that follows the current directives for circular design and resource efficiency in the built environment. The main challenge of reuse is the uniqueness of each salvaged piece, and through our integration featuring detailed data capture about fundamental and intricate features of the component, encompassing geometry and surface detailing with high resolution, effective reuse of reclaimed components is made possible, regardless of how diverse and intricate they are. Owing to the robustness of digitally aided reuse, more components, even the damaged or imperfect ones, can be put back into use instead of being disposed of at landfills or combusted.

Future research will utilize the technological and methodological foundation described in this paper to industrial digital solutions for reuse. It will more deeply dive into the use of generative artificial intelligence (AI), ML, and CV algorithms, to facilitate agile, automated processing of large datasets acquired through element scanning, and further development of automation solutions for the robotic fabrication part, where feature-informed robotic manufacturing and assembly sequences for reuse and renovation can be conducted at industrial scale. In a parallel research project, we are investigating the application of the developed workflows to optimize the robotic 3D printing paths and adapt them to local component features, which adds to a better understanding of the datasets needed for such an application and allows for continued knowledge accumulation concerning more circular practices of architectural reuse, enabled by emerging digital tools and technologies.

## CRedit authorship contribution statement

**Malgorzata A. Zboinska:** Writing – review & editing, Writing – original draft, Visualization, Validation, Supervision, Resources, Project administration, Methodology, Funding acquisition, Formal analysis, Data curation, Conceptualization. **Frederik Göbel:** Writing – review & editing, Visualization, Software, Investigation.



## Declaration of competing interest

The authors declare that they have no known competing financial interests or personal relationships that could have appeared to influence the work reported in this paper.

## Data availability

All code authored by us has been made open source via GitHub and Zenodo, with DOIs provided in the references list below.

## Acknowledgments

This research project was supported by the Digital Twin Cities Centre funded by Sweden's Innovation Agency Vinnova, grant no. 2019-00041.

## References

- [1] United Nations Environment Programme, Global status report for buildings and construction: Beyond foundations – mainstreaming sustainable solutions to cut emissions from the buildings sector, 2023, 2023. <https://wedocs.unep.org/20.500.11822/45095>. Accessed April 29, 2024.
- [2] E. Stricker, G. Brandi, A. Sonderegger, M. Angst, B. Buser, M. Massmünster, Reuse in Construction: A Compendium of Circular Architecture, Park Books, 2022. ISBN 978-3-03860-295-8. <https://www.park-books.com/en/product/reuse-in-construction/46>.
- [3] J. Brütting, G. Senatore, C. Fivet, Form follows availability: designing structures through reuse, *J. Int. Assoc. Shell Spat. Struct.* 60 (4) (2019) 257–265, <https://doi.org/10.20898/j.iaass.2019.202.033>.
- [4] M. Gorgolewski, Resource salvation: the architecture of reuse, John Wiley & Sons (2018), <https://doi.org/10.1002/9781118928806>.
- [5] M. Hughes, Cascading wood, material cycles, and sustainability, in: M. Hudert, S. Pfeiffer (Eds.), *Rethinking Wood: Future Dimensions of Timber Assembly*, Birkhäuser, 2019, pp. 31–46, <https://doi.org/10.1515/9783035617061-002>.
- [6] E. Augustynowicz, N. Aigner, Building from scrap: computational design and robotic fabrication strategies for spatial reciprocal structures from plate-shaped wooden production waste, *J. Archit. Sci. Appl.* 8 (1) (2023) 38–53, <https://doi.org/10.30785/mbud>.
- [7] A. Olumo, J. Zhang, C. Haas, Reality data capture for reclaimed construction materials, in: *The Digital Reality of Tomorrow*, 2022, pp. 1–10, <https://doi.org/10.57922/tcrr.614>.
- [8] S. Çetin, C. De Wolf, N. Bocken, Circular digital built environment: an emerging framework, *Sustainability* 13 (11) (2021) 6348, <https://doi.org/10.3390/su13116348>.
- [9] M. Bügler, A. Borrmann, G. Ogunmakin, P.A. Vela, J. Teizer, Fusion of photogrammetry and video analysis for productivity assessment of earthwork processes, *Comput.-aided civ. Infrastruct. Eng.* 32 (2) (2017) 107–123, <https://doi.org/10.1111/mice.12235>.
- [10] T. Luhmann, Close range photogrammetry for industrial applications, *ISPRS J. Photogramm. Remote Sens.* 65 (6) (2010) 558–569, <https://doi.org/10.1016/j.isprsjprs.2010.06.003>.
- [11] Z. Xiong, M. Gordon, B. Byers, C. De Wolf, Reality capture and site-scanning techniques for material reuse planning, in: *Proceedings of IASS Annual Symposia, IASS/APCS 2022 Beijing Symposium: Sustainable Heritage Challenges and Strategies in the Preservation and Conservation of 20th Century Historic Concrete Shells*, 2022, pp. 1–11, <https://doi.org/10.3929/ethz-b-000580345>.
- [12] N.O. Sönmez, A review of the use of examples for automating architectural design tasks, *Comput. Aided Des.* 96 (2018) 13–30, <https://doi.org/10.1016/j.cad.2017.10.005>.
- [13] M. Tamke, P. Nicholas, M. Zwierzycki, Machine learning for architectural design: practices and infrastructure, *Int. J. Archit. Comput.* 16 (2) (2018) 123–143, <https://doi.org/10.1177/1478077118778580>.
- [14] B. Topuz, N.Ç. Alp, Machine learning in architecture, *Autom. Constr.* 154 (2023) 105012, <https://doi.org/10.1016/j.autcon.2023.105012>.
- [15] M. Ramsgaard Thomsen, P. Nicholas, M. Tamke, S. Gatz, Y. Sinke, G. Rossi, Towards machine learning for architectural fabrication in the age of industry 4.0, *Int. J. Archit. Comput.* 18 (4) (2020) 335–352, <https://doi.org/10.1177/1478077120948000>.
- [16] V. Fragkia, I.W. Foged, A. Pasold, Predictive information modeling: machine learning strategies for material uncertainty, *Technol. Archit. Des.* 5 (2) (2021) 163–176, <https://doi.org/10.1080/24751448.2021.1967057>.
- [17] R. Naboni, L. Breseghello, S. Sanin, Environment-aware 3D concrete printing through robot-vision, in: B. Pak, G. Wurzer, R. Stouffs (Eds.), *Proceedings of the 40th Conference on Education and Research in Computer Aided Architectural Design in Europe, eCAADe and KU Leuven Faculty of Architecture*, 2022, pp. 409–418, <https://doi.org/10.52842/conf.eacaade.2022.2.409>.
- [18] A.A. Apolinaraska, M. Pacher, H. Li, N. Cote, R. Pastrana, F. Gramazio, M. Kohler, Robotic assembly of timber joints using reinforcement learning, *Autom. Constr.* 125 (2021) 103569, <https://doi.org/10.1016/j.autcon.2021.103569>.
- [19] B. Belousov, B. Wibranek, J. Schneider, T. Schneider, G. Chalvatzaki, J. Peters, O. Tessmann, Robotic architectural assembly with tactile skills: simulation and optimization, *Autom. Constr.* 133 (2022) 104006, <https://doi.org/10.1016/j.autcon.2021.104006>.
- [20] P. Nicholas, G. Rossi, E. Williams, M. Bennett, T. Schork, Integrating real-time multi-resolution scanning and machine learning for conformal robotic 3D printing in architecture, *Int. J. Archit. Comput.* 18 (4) (2020) 371–384, <https://doi.org/10.1177/1478077120948203>.
- [21] J. Geno, J. Goosse, S. Van Nimwegen, P. Latteur, Parametric design and robotic fabrication of whole timber reciprocal structures, *Autom. Constr.* 138 (2022) 104198, <https://doi.org/10.1016/j.autcon.2022.104198>.
- [22] A. Kunic, R. Naboni, A. Kramberger, C. Schlette, Design and assembly automation of the robotic reversible timber beam, *Autom. Constr.* 123 (2021) 103531, <https://doi.org/10.1016/j.autcon.2020.103531>.
- [23] R. Rudin, M.A. Zboinska, S. Sämfors, P. Gatenholm, Reprint: A digital workflow for aesthetically retrofitting deteriorated architectural elements with new biomaterial finishes, in: M. Akbarzadeh, D. Aviv, H. Jamelle, R. Stuart-Smith (Eds.), *Hybrids & Haecceities: Proceedings of the 42nd Annual Conference of the Association for Computer Aided Design in Architecture*, 2022, pp. 336–345. ISBN 979-8-9860805-8-1, [https://papers.cumincad.org/data/works/att/acadia22\\_336.pdf](https://papers.cumincad.org/data/works/att/acadia22_336.pdf).
- [24] R. Chiujea, K. Sonne, P. Nicholas, C. Eppinger, M. Ramsgaard Thomsen, Design strategies for repair of 3D printed biocomposite materials, in: N. Gardner, C. M. Herr, L. Wang, H. Toshiaki, S.A. Khan (Eds.), *Accelerated Design: Proceedings of the 29th CAADRIA Conference*, 2024, pp. 311–320. ISBN 978-988-78918-3-3. ISSN 2710-4257 (print). 2710-4265 (online), [https://papers.cumincad.org/data/works/att/caadria2024\\_429.pdf](https://papers.cumincad.org/data/works/att/caadria2024_429.pdf).
- [25] B. Yu, J. Luo, Y. Shi, M. Zhao, A. Fringrut, L. Zhang, Framework for sustainable building design and construction using off-cut wood, *npj Mater Sustain* 1 (2023) 2, <https://doi.org/10.1038/s44296-023-00002-8>.
- [26] C. De Wolf, B.S. Byers, D. Raghu, M. Gordon, V. Schwarzkopf, E. Triantafyllidis, A 5D digital circular workflow: digital transformation towards matchmaking of environmentally sustainable building materials through reuse from disassembly, 2024, <https://doi.org/10.21203/rs.3.rs-4349460/v1> preprint. Accessed August 23, 2024.
- [27] V. Bonora, G. Tucci, A. Meucci, B. Pagnini, Photogrammetry and 3D printing for marble statues replicas: critical issues and assessment, *Sustainability* 13 (2) (2021) 680, <https://doi.org/10.3390/su13020680>.
- [28] M. Higuera, A. Calero, F. Collado-Montero, Digital 3D modelling using photogrammetry and 3D printing applied to the restoration of a Hispano-Roman architectural ornament, *Digit. Appl. Archaeol. Cult. Herit.* 20 (2021) e00179, <https://doi.org/10.1016/j.daach.2021.e00179>.
- [29] I. Salagean-Mohora, A.A. Anghel, F.M. Friguta-Iliasa, Photogrammetry as a digital tool for joining heritage documentation in architectural education and professional practice, *Buildings* 13 (2) (2023) 319, <https://doi.org/10.3390/buildings13020319>.
- [30] J. Xu, L. Ding, P.E.D. Love, Digital reproduction of historical building ornamental components: from 3D scanning to 3D printing, *Autom. Constr.* 76 (2017) 85–96, <https://doi.org/10.1016/j.autcon.2017.01.010>.
- [31] J.M. Wilson, C. Piya, Y.C. Shin, F. Zhao, K. Ramani, Remanufacturing of turbine blades by laser direct deposition with its energy and environmental impact analysis, *J. Clean. Prod.* 80 (2014) 170–178, <https://doi.org/10.1016/j.jclepro.2014.05.084>.
- [32] Y. Zhang, J. Qiao, G. Zhang, H. Tian, L. Li, Artificial intelligence-assisted repair system for structural and electrical restoration using 3D printing, *Adv. Intell. Syst.* 4 (10) (2022) 2200162, <https://doi.org/10.1002/aisy.202200162>.
- [33] J. Yeon, J. Kang, W. Yan, Spall damage repair using 3D printing technology, *Autom. Constr.* 89 (2018) 266–274, <https://doi.org/10.1016/j.autcon.2018.02.003>.
- [34] Y. Wang, G. Ma, L. Wang, W. Zhang, H. Liu, Size effects in cavern model tests based on 3D printing, *Tunn. Undergr. Space Technol.* 137 (2023) 105135, <https://doi.org/10.1016/j.tust.2023.105135>.
- [35] C. Xiang, J. Guo, R. Cao, L. Deng, A crack-segmentation algorithm fusing transformers and convolutional neural networks for complex detection scenarios, *Autom. Constr.* 152 (2023) 104894, <https://doi.org/10.1016/j.autcon.2023.104894>.
- [36] W. Zhang, X. Gu, L. Tang, Y. Yin, D. Liu, Y. Zhang, Application of machine learning, deep learning and optimization algorithms in geoenvironment and geoscience: comprehensive review and future challenge, *Gondwana Res.* 109 (2022) 1–17, <https://doi.org/10.1016/j.jgr.2022.03.015>.
- [37] Robert McNeel & Associates, Rhinoceros 3D. <https://www.rhino3d.com/>.
- [38] D. Rutten, Grasshopper. <https://www.grasshopper3d.com/>.
- [39] J. Wang, KIRI Engine. <https://www.kiriengine.app/>.
- [40] J. Braumann, S. Brell-Cokcan, Association for Robots in Architecture. KUKA|prc. <https://robotsinarchitecture.org/#kukaprc>.
- [41] LucidControl, LucidIo Control .Net Application Programming Interface. <https://www.lucid-control.com/downloads/>.
- [42] F. Göbel, LucidControl. <https://doi.org/10.5281/zenodo.14533735>.
- [43] F. Göbel, Polyga-Grasshopper. <https://doi.org/10.5281/zenodo.1453371>.
- [44] F. Göbel, Better-Data-Recorder. <https://doi.org/10.5281/zenodo.14533728>.
- [45] F. Göbel. <https://doi.org/10.5281/zenodo.14533724>.
- [46] A. Kirillov, E. Mintun, N. Ravi, H. Mao, C. Rolland, L. Gustafson, T. Xiao, S. Whitehead, A.C. Berg, W.-Y. Lo, P. Dollár, R. Girshick, Segment Anything Model (SAM). <https://segment-anything.com/>.
- [47] G. van Rossum. CPython. <https://github.com/python/cpython>.
- [48] E. Iran-Nejad, Grasshopper Hops Python server. <https://github.com/mcneel/compute.rhino3d/tree/8.x/src/ghops-server-py>.
- [49] Intel, Tseez, Willow garage. OpenCV <https://github.com/opencv/opencv>.

- [50] P. Vestartas, A. Settimi. Cockroach. <https://www.food4rhino.com/en/app/cockroach>.
- [51] H. Leander Evers, M. Zwierzycki. Volvox. <https://www.food4rhino.com/en/app/volvox>.
- [52] F. Göbel, Differential-Growth. <https://doi.org/10.5281/zenodo.14533743>.
- [53] M. Zwierzycki, Anemone. <https://www.food4rhino.com/en/app/anemone>.
- [54] R. Oenning, Dendro. <https://www.food4rhino.com/en/app/dendro>.
- [55] T. Brown, B. Mann, N. Ryder, M. Subbiah, J.D. Kaplan, P. Dhariwal, A. Neelakantan, P. Shyam, G. Sastry, A. Askell, S. Agarwal, A. Herbert-Voss, G. Krueger, T. Henighan, R. Child, A. Ramesh, D.M. Ziegler, J. Wu, C. Winter, C. Hesse, M. Chen, E. Sigler, M. Litwin, S. Gray, B. Chess, J. Clark, C. Berner, S. McCandlish, A. Radford, I. Sutskever, D. Amodei, Language models are few-shot learners, in: Advances in Neural Information Processing Systems, 2020, pp. 1877–1901, <https://doi.org/10.48550/arXiv.2005.14165>.
- [56] D. Girardeau-Montaut, R. Janvier, A. Maloney, CloudCompare. <https://www.cloudcompare.org/>.
- [57] W. Liu, Y. Zang, Z. Xiong, X. Bian, C. Wen, X. Lu, C. Wang, J. Marcato Junior, W. Nunes Gonçalves, J. Li, 3D building model generation from MLS point cloud and 3D mesh using multi-source data fusion, Int. J. Appl. Earth Obs. Geoinf. 116 (2023) 103171, <https://doi.org/10.1016/j.jag.2022.103171>.
- [58] C. Jia, T. Yang, C. Wang, B. Fan, F. He, A new fast filtering algorithm for a 3D point cloud based on RGB-D information, PLoS One 14 (8) (2019) e0220253, <https://doi.org/10.1371/journal.pone.0220253>.
- [59] P. Chmelar, L. Rejsek, T.N. Nguyen, D.H. Ha, Advanced methods for point cloud processing and simplification, Appl. Sci. 10 (10) (2020) 3340, <https://doi.org/10.3390/app10103340>.
- [60] D. Zhang, X. Lu, H. Qin, Y. He, Pointfilter: point cloud filtering via encoder-decoder modeling, IEEE Trans. Vis. Comput. 27 (3) (2021) 2015–2027, <https://doi.org/10.1109/TVCG.2020.3027069>.
- [61] D. Muck, H.G. Tomc, U.S. Elesini, M. Ropret, M. Leskoveš, Colour fastness to various agents and dynamic mechanical characteristics of biocomposite filaments and 3D printed samples, Polymers 13 (21) (2021) 3738, <https://doi.org/10.3390/polym13213738>.
- [62] J.A. Travieso-Rodriguez, M.D. Zandi, R. Jerez-Mesa, J. Lluma-Fuentes, Fatigue behavior of PLA-wood composite manufactured by fused filament fabrication, J. Mater. Res. Technol. 9 (4) (2020) 8507–16, doi:<https://doi.org/10.1016/j.jmrt.2020.06.003>.
- [63] M.N. Islam, F. Rahman, A.K. Das, S. Hizirolu, An overview of different types and potential of bio-based adhesives used for wood products, Int. J. Adhes. Adhes. 112 (2022) 102992, <https://doi.org/10.1016/j.ijadhadh.2021.102992>.
- [64] M. Pryor. Pufferfish. <https://www.food4rhino.com/en/app/pufferfish>.
- [65] D. Raghun, M.J.J. Bucher, C. De Wolf, Towards a 'resource cadastre' for a circular economy—urban-scale building material detection using street view imagery and computer vision, Resour. Conserv. Recycl. 198 (2023) 107140, <https://doi.org/10.1016/j.resconrec.2023.107140>.
- [66] B. Yu, A. Fingrut, Sustainable building design (SBD) with reclaimed wood library constructed in collaboration with 3D scanning technology in the UK, Resour. Conserv. Recycl. 186 (2022) 106566, <https://doi.org/10.1016/j.resconrec.2022.106566>.
- [67] J. Aguilar-Camacho, E. Cabrera-Revueita, M. Torres Gonzalez, Comparison of results obtained by photogrammetry tools versus LED handheld scanning technique in architectural heritage, in: B. Tejedor Herrán, D. Bienvenido-Huertas (Eds.), Diagnosis of Heritage Buildings by Non-Destructive Techniques, Woodhead Publishing, 2024, pp. 245–273, <https://doi.org/10.1016/B978-0-443-16001-1.00010-3>.
- [68] A. Murtiyo, P. Grussenmeyer, M. Koehl, T. Freville, Acquisition and processing experiences of close range UAV imagery for the 3D modeling of heritage buildings, in: M. Ioannides, E. Fink, A. Moropoulou, M. Hagedorn-Saupe, A. Fresa, G. Liestøl, V. Rajcic, P. Grussenmeyer (Eds.), Digital Heritage. Progress in Cultural Heritage: Documentation, Preservation, and Protection, 2016, pp. 420–431, [https://doi.org/10.1007/978-3-319-48496-9\\_34](https://doi.org/10.1007/978-3-319-48496-9_34).
- [69] M. Pepe, C. Domenica, Techniques, tools, platforms and algorithms in close range photogrammetry in building 3D model and 2D representation of objects and complex architectures, Comput.-Aided Des Appl. 18 (1) (2020) 42–65, <https://doi.org/10.14733/cadaps.2021.42-65>.
- [70] X. Zhang, M. Li, J.H. Lim, Y. Weng, Y.W.D. Tay, H. Pham, Q.-C. Pham, Large-scale 3D printing by a team of mobile robots, Autom. Constr. 95 (2018) 98–106, <https://doi.org/10.1016/j.autcon.2018.08.004>.
- [71] N. Hack, K. Dörfler, A.N. Walzer, T. Wangler, J. Mata-Falcón, N. Kumar, J. Buchli, W. Kaufmann, R.J. Flatt, F. Gramazio, M. Kohler, Structural stay-in-place formwork for robotic in situ fabrication of nonstandard concrete structures: a real scale architectural demonstrator, Autom. Constr. 115 (2020) 103197, <https://doi.org/10.1016/j.autcon.2020.103197>.
- [72] K.H. Petersen, N. Napp, R. Stuart-Smith, D. Rus, M. Kovac, A review of collective robotic construction, Sci. Robot. 4 (28) (2019), <https://doi.org/10.1126/scirobotics.aau8479> eaa8479.
- [73] M. Yablouina, A. Menges, Towards the development of fabrication machine species for filament materials, in: J. Willmann, P. Block, M. Hutter, K. Byrne, T. Schork (Eds.), Robotic Fabrication in Architecture, Art and Design, 2018, pp. 152–166, [https://doi.org/10.1007/978-3-319-92294-2\\_12](https://doi.org/10.1007/978-3-319-92294-2_12).
- [74] K. Zhang, P. Chermprayong, F. Xiao, D. Tzoumanikas, B. Dams, S. Kay, B.B. Kocer, A. Burns, L. Orr, T. Alhinai, C. Choi, D.D. Darekar, W. Li, S. Hirschmann, V. Soana, S.A. Ngah, C. Grillot, S. Sareh, A. Choubey, L. Margheri, V.M. Pawar, R. J. Ball, C. Williams, P. Shepherd, S. Leutenegger, R. Stuart-Smith, M. Kovac, Aerial additive manufacturing with multiple autonomous robots, Nature 609 (7928) (2022) 709–717, <https://doi.org/10.1038/s41586-022-04988-4>.
- [75] E. Lublasser, T. Adams, A. Vollpracht, S. Brell-Cokcan, Robotic application of foam concrete onto bare wall elements - analysis, concept and robotic experiments, Autom. Constr. 89 (2018) 299–306, <https://doi.org/10.1016/j.autcon.2018.02.005>.
- [76] B. Lu, M. Li, K.F. Leong, S. Qian, M.J. Tan, Develop cementitious materials incorporating fly ash cenosphere for spray-based 3D printing, in: Proceedings of the 3rd International Conference on Progress in Additive Manufacturing, 2018, pp. 38–43, <https://doi.org/10.25341/D4RG6Q>.
- [77] B.G. de Soto, M.J. Skibniewski, Future of robotics and automation in construction, in: A. Sawhney, M. Riley, J. Irizarry (Eds.), Construction 4.0: An Innovation Platform for the Built Environment, Routledge, 2020, pp. 289–306, <https://doi.org/10.1201/9780429398100-15>.
- [78] W. Anane, I. Iordanova, C. Ouellet-Plamondon, BIM-driven computational design for robotic manufacturing in off-site construction: an integrated design-to-manufacturing (DtM) approach, Autom. Constr. 150 (2023) 104782, <https://doi.org/10.1016/j.autcon.2023.104782>.
- [79] P. Bedarf, A. Dutto, M. Zanini, B. Dillenburger, Foam 3D printing for construction: a review of applications, materials, and processes, Autom. Constr. 130 (2021) 103861, <https://doi.org/10.1016/j.autcon.2021.103861>.
- [80] J. Burger, T. Huber, E. Lloret-Fritsch, J. Mata-Falcón, F. Gramazio, M. Kohler, Design and fabrication of optimised ribbed concrete floor slabs using large scale 3D printed formwork, Autom. Constr. 144 (2022) 104599, <https://doi.org/10.1016/j.autcon.2022.104599>.
- [81] S. Mozaffari, M. Bruce, G. Clune, R. Xie, W. McGee, A. Adel, Digital design and fabrication of clay formwork for concrete casting, Autom. Constr. 154 (2023) 104969, <https://doi.org/10.1016/j.autcon.2023.104969>.
- [82] T. Gašpar, M. Deniša, P. Radanović, B. Ridge, T.R. Savarimuthu, A. Kramberger, M. Priggemeyer, J. Roßmann, F. Wörgötter, T. Ivanovska, S. Parizi, Ž. Gosar, I. Kovač, A. Ude, Smart hardware integration with advanced robot programming technologies for efficient reconfiguration of robot workcells, Robot. Comput.-Integr. Manuf. 66 (2020) 101979, <https://doi.org/10.1016/j.rcim.2020.101979>.
- [83] L. Vasey, A. Menges, Potentials of cyber-physical systems in architecture and construction, in: A. Sawhney, M. Riley, J. Irizarry (Eds.), Construction 4.0: An Innovation Platform for the Built Environment, Routledge, 2020, pp. 91–112, <https://doi.org/10.1201/9780429398100-5>.
- [84] J. Braumann, S. Brell-Cokcan, Digital and physical tools for industrial robots in architecture: robotic interaction and interfaces, Int. J. Archit. Comput. 10 (4) (2012) 541–554, <https://doi.org/10.1260/1478-0771.10.4.541>.
- [85] E. Naboni, L. Havinga, Regenerative design in digital practice: a handbook for the built environment, Eur. Res. (2019), <https://doi.org/10.4324/9781003212775>.
- [86] C. De Wolf, S. Çetin, N.M.P. Bocken, A circular built environment in the digital age, Springer Nature (2024), <https://doi.org/10.1007/978-3-031-39675-5>.
- [87] X. Tang, M. Wang, Q. Wang, J. Guo, J. Zhang, Benefits of terrestrial laser scanning for construction QA/QC: a time and cost analysis, J. Manag. Eng. 38 (2) (2022) 05022001, [https://doi.org/10.1061/\(ASCE\)ME.1943-5479.0001012](https://doi.org/10.1061/(ASCE)ME.1943-5479.0001012).
- [88] M. Gordon, L. von Zimmerman, O. Haradthun, D. Campanella, M. Bräutigam, C. De Wolf, Digitising building materials for reuse with reality capture and scan-to-BIM technologies, in: C. De Wolf, S. Çetin, N.M.P. Bocken (Eds.), A Circular Built Environment in the Digital Age, Springer Nature, 2024, pp. 41–55, [https://doi.org/10.1007/978-3-031-39675-5\\_3](https://doi.org/10.1007/978-3-031-39675-5_3).
- [89] M.G. Masciotta, L.J. Sanchez-Aparicio, D.V. Oliveira, D. Gonzalez-Aguilera, Integration of laser scanning technologies and 360° photography for the digital documentation and management of cultural heritage buildings, Int. J. Archit. Herit. 17 (1) (2023) 56–75, <https://doi.org/10.1080/15583058.2022.2069062>.
- [90] Factum Arte. <https://www.factum-arte.com/>.
- [91] Design-to-Production. <https://www.designtoproduction.com/>.
- [92] Hyperion Robotics, <https://www.hyperionrobotics.com/>.
- [93] K. Graser, A. Kahlert, D.M. Hall, DFAB HOUSE: implications of a building-scale demonstrator for adoption of digital fabrication in AEC, Constr. Manag. Econ. 39 (10) (2021) 853–873, <https://doi.org/10.1080/01446193.2021.1988667>.
- [94] F. Craveiro, J.P. Duarte, H. Bartolo, P.J. Bartolo, Additive manufacturing as an enabling technology for digital construction: a perspective on construction 4.0, Autom. Constr. 103 (2019) 251–267, <https://doi.org/10.1016/j.autcon.2019.03.011>.
- [95] P. Das, S. Perera, S. Senaratne, R. Osei-Kyei, Developing a construction business model transformation canvas, Eng. Constr. Archit. Manag. 28 (5) (2021) 1423–1439, <https://doi.org/10.1108/ECAM-09-2020-0712>.
- [96] B.G. de Soto, I. Agustí-Juan, S. Joss, J. Hunhevicz, G. Habert, B. Adey, Rethinking the roles in the AEC industry to accommodate digital fabrication, in: M. J. Skibniewski, M. Hajdu (Eds.), Proceedings of the Creative Construction Conference, 2018, pp. 82–89, <https://doi.org/10.3311/CCC2018-012>.
- [97] V. San Fratello, R. Rael, MUD Frontiers, in: J. Burry, J. Sabin, B. Sheil, M. Skavara (Eds.), Fabricate 2020: Making Resilient Architecture, 2020, pp. 22–27, <https://doi.org/10.2307/j.ctv13xpsv.7>.
- [98] C. Achillas, D. Aidonis, E. Iakovou, M. Thymianidis, D. Tzetzis, A methodological framework for the inclusion of modern additive manufacturing into the production portfolio of a focused factory, J. Manuf. Syst. 37 (1) (2015) 328–339, <https://doi.org/10.1016/j.jmsy.2014.07.014>.
- [99] M. Shuaib, A. Haleem, S. Kumar, M. Javaid, Impact of 3D printing on the environment: a literature-based study, Sustain. Oper. Comput. 2 (2021) 57–63, <https://doi.org/10.1016/j.susoc.2021.04.001>.
- [100] M.R.M. Saade, A. Yahia, B. Amor, How has LCA been applied to 3D printing? A systematic literature review and recommendations for future studies, J. Clean. Prod. 244 (2020) 118803, <https://doi.org/10.1016/j.jclepro.2019.118803>.
- [101] F. Craveiro, H.M. Bartolo, A. Gale, J.P. Duarte, P.J. Bartolo, A design tool for resource-efficient fabrication of 3d-graded structural building components using

- additive manufacturing, *Autom. Constr.* 82 (2017) 75–83, <https://doi.org/10.1016/j.autcon.2017.05.006>.
- [102] I. Agustí-Juan, G. Habert, Environmental design guidelines for digital fabrication, *J. Clean. Prod.* 142 (2017) 2780–2791, <https://doi.org/10.1016/j.jclepro.2016.10.190>.
- [103] N. Labonnote, A. Rönquist, B. Manum, P. Rütther, Additive construction: sState-of-the-art, challenges and opportunities, *Autom. Constr.* 72 (2016) 347–366, <https://doi.org/10.1016/j.autcon.2016.08.026>.
- [104] I. Agustí-Juan, F. Müller, N. Hack, T. Wangler, G. Habert, Potential benefits of digital fabrication for complex structures: environmental assessment of a robotically fabricated concrete wall, *J. Clean. Prod.* 154 (2017) 330–340, <https://doi.org/10.1016/j.jclepro.2017.04.002>.
- [105] I. Krimi, Z. Lafhaj, L. Ducoulombier, Prospective study on the integration of additive manufacturing to building industry—case of a French construction company, *Addit. Manuf.* 16 (2017) 107–114, <https://doi.org/10.1016/j.addma.2017.04.002>.
- [106] M.U. Hossain, S.T. Ng, Influence of waste materials on buildings' life cycle environmental impacts: adopting resource recovery principle, *Resour. Conserv. Recycl.* 142 (2019) 10–23, <https://doi.org/10.1016/j.resconrec.2018.11.010>.
- [107] J. Mehr, C. Vadenbo, B. Steubing, S. Hellweg, Environmentally optimal wood use in Switzerland—investigating the relevance of material cascades, *Resour. Conserv. Recycl.* 131 (2018) 181–191, <https://doi.org/10.1016/j.resconrec.2017.12.026>.
- [108] Y. Niu, K. Rasi, M. Hughes, M. Halme, G. Fink, Prolonging life cycles of construction materials and combating climate change by cascading: the case of reusing timber in Finland, *Resour. Conserv. Recycl.* 170 (2021) 105555, <https://doi.org/10.1016/j.resconrec.2021.105555>.
- [109] I.Z. Bribián, A.V. Capilla, A.A. Usón, Life cycle assessment of building materials: comparative analysis of energy and environmental impacts and evaluation of the eco-efficiency improvement potential, *Build. Environ.* 46 (2011) 1133–1140, <https://doi.org/10.1016/j.buildenv.2010.12.002>.
- [110] V. Hasik, E. Escott, R. Bates, S. Carlisle, B. Faircloth, M.M. Bilec, Comparative whole-building life cycle assessment of renovation and new construction, *Build. Environ.* 161 (2019) 106218, <https://doi.org/10.1016/j.buildenv.2019.106218>.
- [111] U. Kozminska, Circular design: reused materials and the future reuse of building elements in architecture, in: *Process, challenges and case studies*, IOP Conf. Ser.: *Earth Environ. Sci.* 225, 2019, <https://doi.org/10.1088/1755-1315/225/1/012033>, 012033.
- [112] M. Gorgolewski, L. Morettin, The process of designing with reused building components, in: E. Durmisevic (Ed.), *Lifecycle Design of Buildings, Systems and Materials Conference Proceedings*, 2009, pp. 105–109. ISBN 978-90-9024420-4, [https://www.iip.kit.edu/downloads/CIB\\_W115\\_Conference\\_Proceedings\\_Pub\\_323.pdf](https://www.iip.kit.edu/downloads/CIB_W115_Conference_Proceedings_Pub_323.pdf).
- [113] T. Planke, K. Nore, V. Rygh Nordhagen, A. Bockelie, D. Kraniotis, Transformation of reclaimed materials from barn buildings—Design of a new timber building frame, in: A.Q. Nyrud, K.A. Malo, K. Nore (Eds.), *World Conference on Timber Engineering Proceedings*, 2023, pp. 4460–4464, <https://doi.org/10.52202/069179-0581>.
- [114] Y. Huang, L. Alkhatat, C. De Wolf, C. Mueller, Algorithmic circular design with reused structural elements: method and tool, in: C. Fivet, P. D'Acunto, M. Fernandez Ruiz, P.O. Ohlbrock (Eds.), *Proceedings of the International fib Symposium on the Conceptual Design of Structures*, 2021, pp. 457–468, <https://doi.org/10.35789/fib.PROC.0055.2021.CDSymp.P056>.
- [115] G. Celani, Digital fabrication laboratories: pedagogy and impacts on architectural education, *Nexus Network Journal* 14 (3) (2012) 469–482, [https://doi.org/10.1007/978-3-0348-0582-7\\_6](https://doi.org/10.1007/978-3-0348-0582-7_6).
- [116] D. Jenny, H. Mayer, P. Aejmelaeus-Lindström, F. Gramazio, M. Kohler, A pedagogy of digital materiality: integrated design and robotic fabrication projects of the master of advanced studies in architecture and digital fabrication, *Archit. Struct. Constr.* 2 (4) (2022) 649–660, <https://doi.org/10.1007/s44150-022-00040-1>.
- [117] M.A. Zboinska, I. Mjörnell, S. Oguz, R. Rudin, T.S. Dahlstedt, Non-standard robotic 3D printing for architects: a comprehensive digital fabrication lab pedagogy integrating non-programmable material effects, in: B. Pak, G. Wurzer, R. Stouffs (Eds.), *Co-creating the Future: Inclusion in and through Design - Proceedings of the 40th Conference on Education and Research in Computer Aided Architectural Design in Europe*, 2022, pp. 19–28, <https://doi.org/10.52842/conf.eacaade.2022.1.019>.